Signal Processing 188 (2021) 108171

Contents lists available at ScienceDirect

Signal Processing

journal homepage: www.elsevier.com/locate/sigpro

Widely linear FRESH receivers for cancellation of data-like rectilinear and quasi-rectilinear interference with frequency offsets

Pascal Chevalier[a,b], Rémi Chauvat[c], Jean-Pierre Delmas[d,*]

[a] CNAM, laboratory CEDRIC, HESAM University, 292 rue Saint Martin, Paris Cedex 3 75141, France
[b] Thales France, HTE/AMS/TCP, 4 Av. Louvresses, Gennevilliers Cedex 92622, France
[c] TELECOM laboratory, Ecole Nationale de l'Aviation Civile, Toulouse 31400, France
[d] Samovar laboratory, Telecom SudParis, Institut Polytechnique de Paris, Evry Cedex 91011, France

ARTICLE INFO

Article history:
Received 13 October 2020
Revised 8 April 2021
Accepted 27 May 2021
Available online 31 May 2021

Keywords:
Non circular
Widely linear (WL)
SAIC/MAIC
Rectilinear
Quasi-rectilinear
CCI
ISI
ICI
Continous-time
Pseudo-MLSE
FRESH
GMSK
OQAM
VAMOS
FBMC
UAV
CNPC
Frequency offset (FO)

ABSTRACT

Widely linear (WL) receivers have been developed in the past for single antenna interference cancellation (SAIC) of one rectilinear (R) or quasi-rectilinear (QR) data-like multi-user interference (MUI) or co-channel interference (CCI) in particular. The SAIC technology has been implemented in global system for mobile communications (GSM) handsets in particular and has been further analyzed for voice services over adaptive multi-user channels on one slot (VAMOS) standard. It remains of great interest for several current and future applications using R or QR signals, such as anti-collisions processing in radio frequency identification (RFID) or in satellite-AIS systems and to densify 5G and Beyond 5G (B5G) networks through one dimensional signaling or over-loaded large MU-MIMO systems. It may be required to cancel the inter-symbol interference (ISI) of control and non-payload communications (CNPC) links of unmanned aerial vehicles (UAV) and the inter-carrier interference (ICI) of filter bank multi-carrier offset quadrature amplitude modulation (FBMC-OQAM), which are now candidate for B5G mobile networks. For these challenging applications, the development of enhanced WL filtering based SAIC or Multiple Antenna Interference Cancellation (MAIC) receivers for R and QR signals may be of great interest. Such a receiver, corresponding to a three-input WL frequency shift (FRESH) receiver, has been introduced recently for QR signals. However this WL receiver is not robust to a data-like MUI having a residual frequency offset (FO), which occurs for most of the previous applications. In this context, the paper first extends, for arbitrary propagation channels, the standards (for R and QR MUI) and the enhanced (for QR MUI) SAIC/MAIC WL receivers to MUI with a non-zero FO. Then, it shows the less efficiency of the two-input WL receiver for QR MUI with a non-zero FO and the performance improvement obtained with the three-input WL receiver. Finally, it analyzes, both analytically and by simulations, for R and QR MUI, the impact of the MUI FO on the performance of the proposed receivers. The results of the paper should allow the development of new powerful WL receivers for UAV CNPC links, anti-collisions AIS systems and for FBMC-OQAM networks in particular.

1. Introduction

Since more than two decades and the pioneering works on the subject [1–4], WL filtering has raised up a great interest for second-order (SO) non-circular (or improper) [3,5] signals [6–8], in numerous areas, and for MUI mitigation in radiocommunication networks using R or QR modulations in particular. Let us recall that R modulations correspond to mono-dimensional modulations (i.e., with real-valued symbols for digital modulations) such as amplitude modulation (AM), amplitude shift keying (ASK) or binary phase shift keying (BPSK) modulations, whereas QR modulations are complex modulations corresponding, after a simple derotation operation [9], to a complex filtering of a R modulation. Examples of QR modulations are $\pi/2$-BPSK, minimum shift keying (MSK) or OQAM modulations, while an example of approximated QR modulation is the Gaussian MSK (GMSK) modulation.

More precisely, WL processing has been strongly studied and applied for SAIC/MAIC in radio-communication networks using R and QR signals, and in the GSM cellular networks in particular, which use the GMSK modulation. Several SAIC WL receivers, allowing the separation of two users from only one receive antenna,

* Corresponding author.
E-mail addresses: pascal.chevalier@cnam.fr, pascal.chevalier@thalesgroup.com (P. Chevalier), remi.chauvat@recherche.enac.fr (R. Chauvat), jean-pierre.delmas@it-sudparis.eu (J.-P. Delmas).

https://doi.org/10.1016/j.sigpro.2021.108171
0165-1684/

have been proposed in Trigui and Slock [10], Chevalier and Pipon [11], Meyer et al. [12] and inserted in most of GSM handsets since 2006 [13], allowing significant capacity gains in GSM networks [12,14]. Other WL receivers have also been proposed for SAIC [15–17] and SAIC/MAIC [18] in VAMOS networks, a standardized extension of GSM networks, aiming at increasing the capacity of GSM, while maintaining backward compatibility with the legacy system.

Despite these numerous papers about WL processing for R and QR MUI mitigation, this topic remains of great interest for several current and future applications. This concerns in particular anti-collisions processing in Radio Frequency Identification systems [19], which use R signals, and in satellite-AIS systems for maritime surveillance which use GMSK signals [20–22]. This topic is also relevant to allow 5G and B5G networks to support a massive number of low data rate devices through one-dimensional signalling [23] or fully or over-loaded large MU-MIMO systems using R signals [24]. Moreover, QR interference mitigation by WL processing remains also of great interest for Unmanned Aerial Vehicles (UAVs or drones), who are expected to become one of the important enabling technologies for 5G and B5G cellular networks and whose applications development is growing dramatically for many civilian applications (monitoring, surveillance, traffic control, relaying etc..) [25,26]. Indeed, the bidirectional Control and Non Payload Communications (CNPC) link, connecting the ground control station to the UAV, which is a safety-critical link requiring improved receivers in terms of reliability, availability and low latency in a large variety of environmental and propagation conditions, uses the GMSK modulation [27]. In low-altitude operations, CNPC links meet frequency selective wireless channels and WL processing is of interest for channel equalization, as already described recently in Darsena et al. [28]. In order to reduce the size, and then the complexity, of the equalizer, an additional interest of WL processing may be to potentially cancel the multi-paths arriving outside the equalizer length, thus considered as MUI. Another application where QR interference mitigation by WL processing may be still of interest concerns communication networks using FBMC-OQAM waveforms [29], candidate for B5G and future Internet of Things networks [30], thanks to their good frequency localization and compatibility with asynchronous links. For frequency selective channel, FBMC-OQAM waveforms generate Inter-Carrier Interference (ICI) at reception, which may be processed by efficient WL processing. Preliminary WL based solutions for FBMC-OQAM waveforms are presented in Caus and Perez-Neira [31], 32], Chen and Haardt [33] for MIMO links using spatial multiplexing at transmission and in Josilo et al. [34], Ishaque and Ascheid [35] for SISO links. Other applications of the paper may potentially concern SAIC/MAIC of MUI in networks using either DFT-precoded OFDMA systems jointly with GMSK-like modulations for PAPR reduction [36] or CPM modulations, such as MSK modulations, in 1-bit quantization systems [37].

For these challenging applications, the development of enhanced WL filtering based SAIC/MAIC receivers for R and QR signals may be of great interest. For this reason, showing that the standard SAIC/MAIC technology is less powerful for QR signals than for R ones, due to different cyclostationarity and non-circularity properties of these signals, [38] has proposed recently, for QR signals, a SAIC/MAIC enhancement based on a three-input WL FRESH receiver. This new receiver makes QR signals always almost equivalent to R ones for MUI mitigation by WL filtering. Unfortunately, this new receiver does not take into account the potential existence of a residual FO of MUI, necessarily present for most of the applications described above. As it has been shown in Delmas et al. [39] in the GSM context, that standard SAIC/MAIC receivers lose their efficiency if the MUI has a residual FO above a very small fraction of the baud rate, a similar sensitivity to MUI FO should obviously also apply for the enhanced SAIC/MAIC receiver proposed in Chevalier et al. [38].

In this context, the purpose of this paper is fourthfold. The first one is to extend, for R and QR data-like MUI and arbitrary propagation channels, the standard two-input SAIC/MAIC WL receivers to data-like MUI with an arbitrary non-zero residual FO, showing that SAIC/MAIC remains possible in this case. The second purpose of the paper is to show that, for a data-like MUI having a non-zero FO and spectrally overlapping with the SOI, although powerful for R and QR signal, the extended two-input SAIC/MAIC WL receiver is less efficient for QR signals than for R ones. The third purpose of the paper is then to extend, for QR data-like MUI and arbitrary propagation channels, the enhanced three-input SAIC/MAIC WL receiver introduced in Chevalier et al. [38] to data-like MUI with a non-zero residual FO, allowing a SAIC/MAIC improvement with respect to the extended two-input SAIC/MAIC WL receivers. Finally, the fourth purpose of the paper is to analyze, both analytically and by simulations, for both R and QR data-like MUI, the impact of the non-zero MUI FO on the performance of the proposed extended two and three-input WL FRESH receivers. Note that most of the analytical interpretable expressions of the performance of the developed receivers are new and not trivial to develop. They allow a well-understanding of the behaviour of the proposed receivers and are also at the heart of the main contributions of the paper. The results of the paper, mostly original, may contribute to develop elsewhere, for the above applications in particular, new powerful WL receivers for cancellation of ISI and/or MUI with non-zero FO. Note that preliminary results of the paper have been briefly introduced in the conference papers [40,41].

Let us recall that the scarce papers dealing with WL FRESH filtering for equalization/demodulation purposes in the presence of R [42–45] or QR [46–48] CCI do not consider the proposed WL FRESH receivers and do not present any analysis of the residual CCI FO impact on the performance. To the best of our knowledge, the impact of a residual CCI FO on the performance of WL receivers for R or QR data-like MUI has never been analytically analyzed before, to within very partial results presented in Chauvat et al. [40] and Chauvat et al. [41]. This analytical performance analysis, mostly new, is very enlightening in the understanding of the behaviour, the possibilities and the limitations of extended WL FRESH SAIC/MAIC receivers as a function of the residual MUI FO.

The paper is organized as follows. Section 2 introduces the observation model, the extended two-input (for R and QR MUI) and three-input (for QR MUI) FRESH models for WL processing in the presence of a data-like MUI with a non-zero residual FO, jointly with the SO statistics of the total noise. Section 3 introduces the conventional linear and the extended two and three-input WL FRESH receivers for the demodulation of R and QR signals in the presence of one data-like MUI with residual FO. Section 4 presents, for several propagation channels, in the presence of one data-like MUI with a non-zero FO and in terms of output signal to interference plus noise ratio (SINR) on the current symbol, a comparative performance analysis of SAIC/MAIC from the proposed extended two-input (for R and QR MUI) and three-input (for QR MUI) WL FRESH receivers. Section 5 shows that the results obtained through the output SINR criterion are still valid for the output symbol error rate (SER). Finally Section 6 concludes this paper.

Notations: Before proceeding, we fix the notations used throughout the paper. Non boldface symbols are scalar whereas lower (upper) case boldface symbols denote column vectors (matrices). T, H and $*$ means the transpose, conjugate transpose and conjugate, respectively. The complex number i is such that $i^2=-1$ and $i^\ell=e^{i\ell\pi/2}$, $\delta(x)$ and $\mathbb{1}_C(x)$ are the Kronecker symbol and indicator function, respectively such that $\delta(x)=1$ for $x=0$ and $\delta(x)=0$ for $x\neq 0$, $\mathbb{1}_C(x)=1$ if $x\in C$ and $\mathbb{1}_C(x)=0$ if $x\notin C$. Moreover, all Fourier transforms of vectors $\mathbf{x}$ and matrices $\mathbf{X}$ use the same notation where time parameters t or τ is simply replaced by frequency f.

Table 1
Acronymes.

AIS	Automatic Identification System	MLSE	Maximum Likelihood Sequence Estimation
AM	Amplitude Modulation	MMSE	Minimum Mean Square Error
ASK	Amplitude Shift Keying	MSK	Minimum Shift Keying
B5G	Beyond 5G	MUI	Multi-User Interference
BPSK	Binary Phase Shift Keying	OQAM	Offset Quadrature Amplitude Modulation
CCI	Co-Channel Interference	QR	Quasi-Rectilinear
CNPC	Control and Non Payload Communication	R	Rectilinear
CT	Continuous Time	RFID	Radio-Frequency Identification
DT	Discrete Time	SAIC	Single Antenna Interference Cancellation
FBMC	Filter-Bank Multicarrier	SER	Symbol Error Rate
FO	Frequency Offset	SINR	Signal to Interference plus Noise Ratio
FRESH	Frequency Shifted	SISO	Single Input Single Output
GMSK	Gaussian Minimum Shift Keying	SO	Second Order
ICI	Intercarrier Interference	SOI	Signal of Interest
ISI	Intersymbol Interference	SRRC	Square Root Raised Cosine
MAIC	Multiple Antenna Interference Cancellation	VAMOS	Voice Services over Adaptive Multi-user channel on one slot
MIMO	Multiple Input Multiple Output	WL	Widely Linear

2. Models and total noise second-order statistics

2.1. Observation model and total noise SO statistics

We consider an array of N narrow-band antennas receiving the contribution of a SOI, which may be R or QR, one data-like multi-user CCI, having the same nature (R or QR), the same symbol period and the same pulse-shaping filter as the SOI, and a background noise. The $N\times 1$ vector of complex amplitudes of the data at the output of these antennas after frequency synchronization can then be written as

$$\begin{aligned}\mathbf{x}(t) &= \sum_{\ell} a_\ell \mathbf{g}(t-\ell T) + \sum_{\ell} c_\ell [v(t-\ell T)e^{i2\pi\Delta_f t}]\otimes \mathbf{h}_I(t) + \mathbf{u}(t)\\ &= \sum_{\ell} a_\ell \mathbf{g}(t-\ell T) + \sum_{\ell} c_\ell e^{i2\pi\Delta_f \ell T}\mathbf{g}_{I_0}(t-\ell T) + \mathbf{u}(t)\\ &= \sum_{\ell} a_\ell \mathbf{g}(t-\ell T) + \mathbf{n}(t). \end{aligned} \tag{1}$$

Here, $(a_\ell, c_\ell) = (b_\ell, d_\ell)$ for R signals, whereas $(a_\ell, c_\ell) = (i^\ell b_\ell, i^\ell d_\ell)$ for QR signals, where b_ℓ and d_ℓ are real-valued zero-mean independent identically distributed (i.i.d.) random variables, corresponding to the SOI and CCI symbols respectively for R signals and directly related to the SOI and CCI symbols, respectively for QR signals [43,45], T is the symbol period for R, $\pi/2$-BPSK, MSK and GMSK signals [50,51] and half the symbol period for OQAM signals [49], $\mathbf{g}(t) = v(t)\otimes \mathbf{h}(t)$ is the $N\times 1$ impulse response of the SOI global channel, $\otimes$ is the convolution operation, $v(t)$ and $\mathbf{h}(t)$ are respectively the scalar and $N\times 1$ impulse responses of the SOI pulse shaping filter and propagation channel, respectively, Δ_f is the residual FO of the CCI, which is assumed to be known or perfectly estimated a priori, $\mathbf{g}_{I_0}(t) \overset{\text{def}}{=} v_o(t)\otimes \mathbf{h}_I(t)$ where $v_o(t) \overset{\text{def}}{=} v(t)e^{i2\pi\Delta_f t}$ is the frequency shifted or offsetted $v(t)$ and $\mathbf{h}_I(t)$ is the impulse response of the propagation channel of the CCI, $\mathbf{u}(t)$ is the $N\times 1$ background noise vector assumed zero-mean, circular, stationary, temporally and spatially white and $\mathbf{n}(t)$ is the total noise vector composed of the CCI and background noise. Note that model (1) with $(a_\ell, c_\ell) = (i^\ell b_\ell, i^\ell d_\ell)$ is exact for $\pi/2$-BPSK, MSK and OQAM signals whereas it is only an approximated model for GMSK signals [50].

The SO statistics of $\mathbf{n}(t)$ are characterized by the two correlation matrices $\mathbf{R}_n(t,\tau)$ and $\mathbf{C}_n(t,\tau)$, defined by

$$\mathbf{R}_n(t,\tau) \overset{\text{def}}{=} \mathrm{E}[\mathbf{n}(t+\tau/2)\mathbf{n}^H(t-\tau/2)] \tag{2}$$

$$\mathbf{C}_n(t,\tau) \overset{\text{def}}{=} \mathrm{E}[\mathbf{n}(t+\tau/2)\mathbf{n}^T(t-\tau/2)]. \tag{3}$$

Using (1) and the relation $[j(t)e^{i2\pi\Delta_f t}]\otimes \mathbf{h}_I(t) = e^{i2\pi\Delta_f t}[j(t)\otimes \mathbf{h}'_I(t)]$ with $\mathbf{h}'_I(t) \overset{\text{def}}{=} \mathbf{h}_I(t)e^{-i2\pi\Delta_f t}$, where $j(t)$ is the baseband signal of the CCI, it is easy to verify that for both R and QR signals, $\mathbf{R}_n(t,\tau)$ is a periodic function of t with a period equal to T. In a same way, it is easy to show that $\mathbf{C}_n(t,\tau) = \mathbf{C}'_n(t,\tau)e^{i4\pi\Delta_f t}$ where $\mathbf{C}'_n(t,\tau)$ is a periodic function of t with a period equal to T and $2T$ for R and QR signals respectively. Matrices $\mathbf{R}_n(t,\tau)$ and $\mathbf{C}_n(t,\tau)$ have then Fourier series expansions given by

$$\mathbf{R}_n(t,\tau) = \sum_{\alpha_k} \mathbf{R}_n^{\alpha_k}(\tau)e^{i2\pi\alpha_k t} \tag{4}$$

$$\mathbf{C}_n(t,\tau) = \sum_{\beta_k} \mathbf{C}_n^{\beta_k}(\tau)e^{i2\pi\beta_k t}. \tag{5}$$

Here, α_k and β_k are the so-called non-conjugate and conjugate SO cyclic frequencies of $\mathbf{n}(t)$, such that $\alpha_k = k/T\,(k\in\mathbb{Z})$ for both R and QR signals, whereas $\beta_k = 2\Delta_f + k/T$ and $\beta_k = 2\Delta_f + (2k+1)/2T$, $(k\in\mathbb{Z})$ for R and QR signals, respectively [52], $\mathbf{R}_n^{\alpha_k}(\tau)$ and $\mathbf{C}_n^{\beta_k}(\tau)$ are respectively the first and second cyclic correlation matrices of $\mathbf{n}(t)$ for the cyclic frequencies α_k and β_k and the delay τ, defined by

$$\mathbf{R}_n^{\alpha_k}(\tau) \overset{\text{def}}{=} \langle \mathbf{R}_n(t,\tau)e^{-i2\pi\alpha_k t}\rangle \tag{6}$$

$$\mathbf{C}_n^{\beta_k}(\tau) \overset{\text{def}}{=} \langle \mathbf{C}_n(t,\tau)e^{-i2\pi\beta_k t}\rangle, \tag{7}$$

where $\langle . \rangle$ is the temporal mean operation in t over an infinite observation duration. The Fourier transforms $\mathbf{R}_n^{\alpha_k}(f)$ and $\mathbf{C}_n^{\beta_k}(f)$ of $\mathbf{R}_n^{\alpha_k}(\tau)$ and $\mathbf{C}_n^{\beta_k}(\tau)$, respectively, are called the first and second cyclospectrum of $\mathbf{n}(t)$ for the cyclic frequencies α_k and β_k, respectively. Note that the first and second cyclospectrum of the transmitted SOI

$$s(t) \overset{\text{def}}{=} \sum_{\ell} a_\ell v(t-\ell T), \tag{8}$$

for the cyclic frequencies α_k and β_k, respectively, denoted by $r_s^{\alpha_k}(f)$ and $c_s^{\beta_k}(f)$, respectively, are given, after elementary computations, for both R and QR SOI, by the expressions

$$r_s^{\alpha_k}(f) = (\pi_b/T)v(f+\alpha_k/2)v^*(f-\alpha_k/2) \tag{9}$$

$$c_s^{\beta_k}(f) = (\pi_b/T)v(f+\beta_k/2)v(\beta_k/2-f), \tag{10}$$

where $\pi_b \overset{\text{def}}{=} \mathrm{E}(b_k^2)$.

2.2. Extended two-input and three-input FRESH models for WL processing with CCI FO

2.2.1. Conventional linear processing

For both R and QR signals, a conventional linear processing of $\mathbf{x}(t)$ only exploits the information contained at the zero non-conjugate ($\alpha = 0$) SO cyclic frequency of $\mathbf{x}(t)$, through the exploitation of the temporal mean of the first correlation matrix, $\mathbf{R}_x(t,\tau) \overset{\text{def}}{=} \mathrm{E}[\mathbf{x}(t+\tau/2)\mathbf{x}^H(t-\tau/2)]$, of $\mathbf{x}(t)$.

2.2.2. Extended two-input FRESH model for WL processing of R signals

For R signals, a standard WL processing of $\mathbf{x}(t)$, i.e. a linear processing of the two-input model $\widetilde{\mathbf{x}}(t) \overset{\text{def}}{=} [\mathbf{x}^T(t), \mathbf{x}^H(t)]^T$, only exploits the information contained at the zero non-conjugate and conjugate $(\alpha,\beta) = (0,0)$ SO cyclic frequencies of $\mathbf{x}(t)$ through the exploitation of the temporal mean of the first correlation matrix, $\mathbf{R}_{\widetilde{x}}(t,\tau) \overset{\text{def}}{=} \mathrm{E}[\widetilde{\mathbf{x}}(t+\tau/2)\widetilde{\mathbf{x}}^H(t-\tau/2)]$, of $\widetilde{\mathbf{x}}(t)$. However, in the presence of a non-zero FO, the most energetic conjugate SO cyclic frequency of an R CCI is $\beta_0 = 2\Delta_f$, which is non-zero for $\Delta_f \neq 0$. For this reason, standard WL processing of $\mathbf{x}(t)$, and thus standard SAIC/MAIC receivers [10–12], give generally degraded performance for $\Delta_f \neq 0$, which even correspond to the conventional ones if no energy is present at $\beta = 0$, i.e., if $\Delta_f \neq k/2T (k \in \mathbb{Z})$. To be efficient in all cases in the presence of a CCI with a non-zero FO, SAIC/MAIC receivers have to exploit the information contained in $\beta_0 = 2\Delta_f$. Using the results of [2], we deduce that this can be done, whatever the value of Δ_f, through the exploitation of the extended two-input FRESH observation vector $\mathbf{x}_{R_{F_2}}(t) \overset{\text{def}}{=} [\mathbf{x}^T(t), e^{i4\pi\Delta_f t}\mathbf{x}^H(t)]^T$, given by

$$\mathbf{x}_{R_{F_2}}(t) = \sum_\ell b_\ell \mathbf{g}_{R_{F_2},\ell}(t-\ell T) + \mathbf{n}_{R_{F_2}}(t), \tag{11}$$

where $\mathbf{g}_{R_{F_2},\ell}(t) \overset{\text{def}}{=} [\mathbf{g}^T(t), e^{i4\pi\Delta_f(t+\ell T)}\mathbf{g}^H(t)]^T$ and $\mathbf{n}_{R_{F_2}}(t) \overset{\text{def}}{=} [\mathbf{n}^T(t), e^{i4\pi\Delta_f t}\mathbf{n}^H(t)]^T$. It is straightforward to verify that the temporal mean of the first correlation matrix, $\mathbf{R}_{x_{R_{F_2}}}(t,\tau) \overset{\text{def}}{=} \mathrm{E}[\mathbf{x}_{R_{F_2}}(t+\tau/2)\mathbf{x}^H_{R_{F_2}}(t-\tau/2)]$, of $\mathbf{x}_{R_{F_2}}(t)$ exploits the information contained in $(\alpha,\beta) = (0, 2\Delta_f)$.

2.2.3. Extended two and three-input FRESH models for WL processing of QR signals

For QR signals with a zero FO, as no information is contained at $\beta = 0$, a derotation preprocessing of the data is required before standard WL processing. Using (1) for QR signals, the derotated observation vector can be written as

$$\mathbf{x}_d(t) \overset{\text{def}}{=} i^{-t/T}\mathbf{x}(t) = \sum_\ell b_\ell \mathbf{g}_d(t-\ell T) + \mathbf{n}_d(t) \tag{12}$$

where $\mathbf{g}_d(t) \overset{\text{def}}{=} i^{-t/T}\mathbf{g}(t)$ and $\mathbf{n}_d(t) \overset{\text{def}}{=} i^{-t/T}\mathbf{n}(t)$. Eq. (12) shows that the derotation operation makes a QR signal looks like an R signal, with non-conjugate, α_{d_k}, and conjugate, β_{d_k}, SO cyclic frequencies equal to $\alpha_{d_k} = \alpha_k = k/T$ and $\beta_{d_k} = \beta_k - 1/2T = k/T$ [38], which proves the presence of information at $\beta_d = 0$. Then, standard WL processing of QR signals, which corresponds to standard WL processing of $\mathbf{x}_d(t)$, i.e. to linear processing of $\widetilde{\mathbf{x}}_d(t) \overset{\text{def}}{=} [\mathbf{x}_d^T(t), \mathbf{x}_d^H(t)]^T$, exploits the information contained at the zero non-conjugate and conjugate $(\alpha_d,\beta_d) = (0,0)$ SO cyclic frequencies of $\mathbf{x}_d(t)$ or equivalently at the SO cyclic frequencies $(\alpha,\beta) = (0, 1/2T)$ of $\mathbf{x}(t)$. This is done through the exploitation of the temporal mean of the first correlation matrix, $\mathbf{R}_{\widetilde{x}_d}(t,\tau) \overset{\text{def}}{=} \mathrm{E}[\widetilde{\mathbf{x}}_d(t+\tau/2)\widetilde{\mathbf{x}}_d^H(t-\tau/2)]$, of $\widetilde{\mathbf{x}}_d(t)$ or equivalently, of the first correlation matrix, $\mathbf{R}_{x_{QR_2}}(t,\tau) \overset{\text{def}}{=} \mathrm{E}[\mathbf{x}_{QR_2}(t+\tau/2)\mathbf{x}^H_{QR_2}(t-\tau/2)]$, of the two-input FRESH model $\mathbf{x}_{QR_2}(t) \overset{\text{def}}{=} [\mathbf{x}^T(t), e^{i2\pi t/2T}\mathbf{x}^H(t)]^T = i^{t/T}\widetilde{\mathbf{x}}_d(t)$.

Nevertheless, for $\Delta_f = 0$, contrary to R CCI, a QR CCI has two most energetic conjugate SO cyclic frequencies corresponding to $(\beta_{d_0}, \beta_{d_{-1}}) = (0, -1/T)$, if the CCI is derotated, and to $(\beta_0, \beta_{-1}) = (1/2T, -1/2T)$ without any derotation [52]. This proves the sub-optimality of the two-input model, $\widetilde{\mathbf{x}}_d(t)$ or $\mathbf{x}_{QR_2}(t)$, for QR signals, discussed in details in Chevalier et al. [38], which only exploits one of these two cyclic frequencies, $\beta_d = 0$ or $\beta = 1/2T$. This sub-optimality explains why standard WL filtering may be less efficient for QR signals than for R ones as proved in Chevalier et al. [38]. To overcome this limitation, and to make QR signals at least almost equivalent to R ones for WL filtering without any FO, a three-input FRESH model, $\mathbf{x}_{d_3}(t) \overset{\text{def}}{=} [\widetilde{\mathbf{x}}_d^T(t), e^{-i2\pi t/T}\mathbf{x}_d^H(t)]^T$, or equivalently $\mathbf{x}_{QR_3}(t) \overset{\text{def}}{=} [\mathbf{x}^T(t), e^{i2\pi t/2T}\mathbf{x}^H(t), e^{-i2\pi t/2T}\mathbf{x}^H(t)]^T = i^{t/T}\mathbf{x}_{d_3}(t)$, has been introduced in Chevalier et al. [38] for QR signals. It is straightforward to verify that the temporal mean of the first correlation matrix of $\mathbf{x}_{d_3}(t)$ and $\mathbf{x}_{QR_3}(t)$ exploit the information contained in $(\alpha_{d_0}, \alpha_{d_{-1}}, \alpha_{d_1}, \beta_{d_0}, \beta_{d_{-1}}) = (0, -1/T, 1/T, 0, -1/T)$ and in $(\alpha_0, \alpha_{-1}, \alpha_1, \beta_0, \beta_{-1}) = (0, -1/T, 1/T, 1/2T, -1/2T)$ respectively, which allows us to exploit almost exhaustively both the SO cyclostationarity and the SO non-circularity properties of QR signals.

However, for $\Delta_f \neq 0$, the two most energetic conjugate SO cyclic frequency of a QR CCI are $(\beta_{d_0}, \beta_{d_{-1}}) = (2\Delta_f, 2\Delta_f - 1/T)$, if the CCI is derotated, and $(\beta_0, \beta_{-1}) = (2\Delta_f + 1/2T, 2\Delta_f - 1/2T)$ without any derotation [52]. As $\beta_{d_k} \neq 0$ for $\Delta_f \neq \ell/2T$, where k and ℓ are integers, standard WL receivers for QR signals give the performance of conventional ones for $\Delta_f \neq \ell/2T$. To be efficient in the presence of a QR CCI with an arbitrary FO, two-input SAIC/MAIC receivers have to exploit the information contained in either $\beta_{d_0} = 2\Delta_f$ (or $\beta_0 = 2\Delta_f + 1/2T$) or $\beta_{d_{-1}} = 2\Delta_f - 1/T$ (or $\beta_{-1} = 2\Delta_f - 1/2T$). Similarly, the three-input SAIC/MAIC receiver has to exploit the information contained in both $\beta_{d_0} = 2\Delta_f$ and $\beta_{d_{-1}} = 2\Delta_f - 1/T$ (or $\beta = 2\Delta_f \pm 1/2T$). Using the results of [2], we deduce that, for a QR CCI with an arbitrary non zero FO, the extended two and three-input WL FRESH receivers have to exploit the extended two and three-input FRESH observation vectors, $\mathbf{x}_{QR_{F_2}}(t)$ and $\mathbf{x}_{QR_{F_3}}(t)$ respectively, defined by

$$\begin{aligned}\mathbf{x}_{QR_{F_2}}(t) &\overset{\text{def}}{=} [\mathbf{x}^T(t), e^{i2\pi(2\Delta_f+1/2T)t}\mathbf{x}^H(t)]^T \\ &= i^{t/T}[\mathbf{x}_d^T(t), e^{i4\pi\Delta_f t}\mathbf{x}_d^H(t)]^T \\ &= \sum_\ell i^\ell b_\ell \mathbf{g}_{QR_{F_2},\ell}(t-\ell T) + \mathbf{n}_{QR_{F_2}}(t),\end{aligned} \tag{13}$$

$$\begin{aligned}\mathbf{x}_{QR_{F_3}}(t) &\overset{\text{def}}{=} [\mathbf{x}^T(t), e^{i2\pi(2\Delta_f+1/2T)t}\mathbf{x}^H(t), e^{i2\pi(2\Delta_f-1/2T)t}\mathbf{x}^H(t)]^T \\ &= i^{t/T}[\mathbf{x}_d^T(t), e^{i4\pi\Delta_f t}\mathbf{x}_d^H(t), e^{i4\pi(\Delta_f-1/2T)t}\mathbf{x}_d^H(t)]^T \\ &= \sum_\ell i^\ell b_\ell \mathbf{g}_{QR_{F_3},\ell}(t-\ell T) + \mathbf{n}_{QR_{F_3}}(t),\end{aligned} \tag{14}$$

where $\mathbf{g}_{QR_{F_2},\ell}(t) \overset{\text{def}}{=} [\mathbf{g}^T(t), e^{i4\pi\Delta_f\ell T}e^{i2\pi(2\Delta_f+1/2T)t}\mathbf{g}^H(t)]^T$, $\mathbf{g}_{QR_{F_3},\ell}(t) \overset{\text{def}}{=} [\mathbf{g}^T(t), e^{i4\pi\Delta_f\ell T}e^{i2\pi(2\Delta_f+1/2T)t}\mathbf{g}^H(t), e^{i4\pi\Delta_f\ell T}e^{i2\pi(2\Delta_f-1/2T)t}\mathbf{g}^H(t)]^T$, $\mathbf{n}_{QR_{F_2}}(t) \overset{\text{def}}{=} [\mathbf{n}^T(t), e^{i2\pi(2\Delta_f+1/2T)t}\mathbf{n}^H(t)]^T$ and $\mathbf{n}_{QR_{F_3}}(t) \overset{\text{def}}{=} [\mathbf{n}^T(t), e^{i2\pi(2\Delta_f+1/2T)t}\mathbf{n}^H(t), e^{i2\pi(2\Delta_f-1/2T)t}\mathbf{n}^H(t)]^T$. It is straightforward to verify that the temporal mean of the first correlation matrix, $\mathbf{R}_{x_{QR_{F_2}}}(t,\tau) \overset{\text{def}}{=} \mathrm{E}[\mathbf{x}_{QR_{F_2}}(t+\tau/2)\mathbf{x}^H_{QR_{F_2}}(t-\tau/2)]$, of $\mathbf{x}_{QR_{F_2}}(t)$ exploits the information contained in $(\alpha_0,\beta_0) = (0, 2\Delta_f + 1/2T)$. Similarly, the temporal mean of the first correlation matrix, $\mathbf{R}_{x_{QR_{F_3}}}(t,\tau) \overset{\text{def}}{=} \mathrm{E}[\mathbf{x}_{QR_{F_3}}(t+\tau/2)\mathbf{x}^H_{QR_{F_3}}(t-\tau/2)]$, of $\mathbf{x}_{QR_{F_3}}(t)$ exploits the information contained in $(\alpha_0, \alpha_{-1}, \alpha_1, \beta_0, \beta_{-1}) = (0, -1/T, 1/T, 2\Delta_f + 1/2T, 2\Delta_f - 1/2T)$.

3. Generic extended pseudo-MLSE receiver

3.1. Pseudo-MLSE approach

To extend, in an efficient original way and for an arbitrary propagation channel, the two-input (for R and QR CCI) and the three-input (for QR CCI) SAIC/MAIC receivers for CCI with a non-zero FO, and to analyze the impact of this FO on the performance, we use the continuous-time (CT) pseudo-maximum likelihood sequence estimation (pseudo-MLSE) approach introduced recently in Chevalier et al. [38]. Then we apply it to the extended models (11) (for R CCI) and (13) and (14) (for QR CCI), respectively. This approach consists in computing the CT MLSE receiver from extended models (11), (13) and (14), respectively, assuming that the associated total noise $\mathbf{n}_{R_{F_2}}(t)$, $\mathbf{n}_{QR_{F_2}}(t)$ and $\mathbf{n}_{QR_{F_3}}(t)$, respectively, is Gaussian, circular and stationary. Such an approach is much easier to manipulate than an MLSE approach for a cyclostationary total noise, is more powerful than a minimum mean square error (MMSE) approach and allows us to remove, both the filtering structure constraints generally imposed by a discrete time (DT) approach and the potential influence of the sample rate. Moreover, it allows us to obtain analytical interpretable performance computations at the output of all the receivers considered in this paper, which is completely original. Note that the conventional CT pseudo-MLSE receiver, called CT one-input pseudo MLSE receiver, corresponds to the CT MLSE receiver computed from $\mathbf{x}(t)$, assuming a Gaussian circular and stationary total noise $\mathbf{n}(t)$.

3.2. Generic extended pseudo-MLSE receiver

We denote by $\mathbf{x}_{F_M}(t)$ and $\mathbf{n}_{F_M}(t)$ the generic extended M-input ($M=1,2$ for R signals and $M=1,2,3$ for QR signals) FRESH observation and total noise vectors, respectively. For conventional receivers ($M=1$), $\mathbf{x}_{F_1}(t)$ and $\mathbf{n}_{F_1}(t)$ reduce to $\mathbf{x}(t)$ and $\mathbf{n}(t)$, respectively for both R and QR signals. For $M=2$, $\mathbf{x}_{F_2}(t)$ and $\mathbf{n}_{F_2}(t)$ correspond, for R signals, to $\mathbf{x}_{R_{F_2}}(t)$ and $\mathbf{n}_{R_{F_2}}(t)$, respectively, defined by (11), and for QR signals, to $\mathbf{x}_{QR_{F_2}}(t)$ and $\mathbf{n}_{QR_{F_2}}(t)$, respectively, defined by (13). For $M=3$, $\mathbf{x}_{F_3}(t)$ and $\mathbf{n}_{F_3}(t)$ correspond, for QR signals, to $\mathbf{x}_{QR_{F_3}}(t)$ and $\mathbf{n}_{QR_{F_3}}(t)$ respectively, defined by (14). Assuming a stationary, circular and Gaussian generic extended M-input total noise $\mathbf{n}_{F_M}(t)$, it is shown in Sallem et al. [53], Ungerboeck [54] that the sequence $\mathbf{b} \overset{\text{def}}{=} (b_1,\ldots,b_K)$ which maximizes its likelihood from $\mathbf{x}_{F_M}(t)$, is the one which minimizes the following criterion:

$$C(\mathbf{b}) = \int [\mathbf{x}_{F_M}(f)-\mathbf{s}_{F_M}(f)]^H [\mathbf{R}^0_{n_{F_M}}(f)]^{-1}[\mathbf{x}_{F_M}(f)-\mathbf{s}_{F_M}(f)]df. \tag{15}$$

Here, $\mathbf{R}^0_{n_{F_M}}(f)$, the Fourier transform of $\mathbf{R}^0_{n_{F_M}}(\tau)$, corresponds to the power spectral density matrix of $\mathbf{n}_{F_M}(t)$. The Fourier transform $\mathbf{s}_{F_M}(f)$ is defined by $\mathbf{s}_{F_M}(f) \overset{\text{def}}{=} \sum_{\ell=1}^K a_\ell \mathbf{g}_{F_M,\ell}(f)e^{-i2\pi f\ell T}$, where $\mathbf{g}_{F_M,\ell}(f)$ corresponds, for $M=1$, to $\mathbf{g}(f)$ for R and QR signals, for $M=2$, to $\mathbf{g}_{R_{F_2},\ell}(f)$ and $\mathbf{g}_{QR_{F_2},\ell}(f)$ for R and QR signals, respectively and for $M=3$, to $\mathbf{g}_{QR_{F_3},\ell}(f)$ for QR signals, whereas $a_\ell = b_\ell$ for R signals and $a_\ell = i^\ell b_\ell$ for QR signals. Considering only terms that depend on the symbols b_ℓ, the minimization of (15) is equivalent to the minimization of the metric:

$$\Lambda(\mathbf{b}) = \sum_{\ell=1}^K \sum_{\ell'=1}^K b_\ell b_{\ell'} r_{\ell,\ell'} - 2\sum_{\ell=1}^K b_\ell z_{F_M}(\ell), \tag{16}$$

where $z_{F_M}(\ell) = \text{Re}[y_{F_M}(\ell)]$ for R signals, $z_{F_M}(\ell) = \text{Re}[i^{-\ell}y_{F_M}(\ell)]$ for QR signals and where $y_{F_M}(\ell)$ and the coefficients $r_{\ell,\ell'}$ are defined by

$$y_{F_M}(\ell) = \int \mathbf{g}^H_{F_M,\ell}(f)[\mathbf{R}^0_{n_{F_M}}(f)]^{-1}\mathbf{x}_{F_M}(f)e^{i2\pi f\ell T}df \tag{17}$$

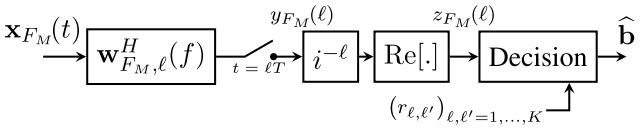

Fig. 1. Structure of the extended M-input ($M=1,2,3$) pseudo-MLSE receiver (for QR signals).

$$r_{\ell,\ell'} = \epsilon_{\ell,\ell'}\int \mathbf{g}^H_{F_M,\ell}(f)[\mathbf{R}^0_{n_{F_M}}(f)]^{-1}\mathbf{g}_{F_M,\ell'}(f)e^{i2\pi f(\ell-\ell')T}df, \tag{18}$$

where $\epsilon_{\ell,\ell'}=1$ for R signals and $\epsilon_{\ell,\ell'} = i^{\ell'-\ell}$ for QR signals.

3.3. Interpretation of the generic extended pseudo-MLSE receiver

We deduce from (17) that $y_{F_M}(\ell)$ is the sampled output, at time $t=\ell T$, of the filter whose frequency response is

$$\mathbf{w}^H_{F_M,\ell}(f) \overset{\text{def}}{=} \left([\mathbf{R}^0_{n_{F_M}}(f)]^{-1}\mathbf{g}_{F_M,\ell}(f)\right)^H, \tag{19}$$

and whose input is $\mathbf{x}_{F_M}(t)$. The structure of the generic extended M-input pseudo-MLSE receiver ($M=1,2,3$) is then depicted at Fig. 1. It is composed of the extended M-input filter (19), which reduces to a time invariant linear filter for $M=1$, followed by a sampling at the symbol rate, a derotation operation (for QR signals), a real part capture[1] and a decision box implementing the Viterbi algorithm, since $r^*_{\ell,\ell'} = r_{\ell',\ell}$.

3.4. Implementation of the generic extended generic pseudo-MLSE receiver

The implementation of the generic extended M-input ($M=1,2,3$) pseudo-MLSE receiver requires the knowledge or the estimation of $\mathbf{g}_{F_M,\ell}(f)$ and $\mathbf{R}^0_{n_{F_M}}(f)$ for each frequency f. This implementation is out of the scope of the paper but it requires the estimation of the channel impulse response of both the SOI and the CCI and the estimation of the background noise power spectral density.

3.5. SINR at the output of the generic extended pseudo-MLSE receiver

For real-valued symbols b_ℓ, the SER at the output of the generic extended M-input ($M=1,2,3$) pseudo-MLSE receiver is directly linked to the SINRs on the current symbol m before decision, i.e., at the output $z_{F_M}(m)$ [51, Sec 10.1.4], without taking into account the ISI which is processed by the decision box. For this reason, we compute the general expression of the output SINRs hereafter and we will analyze their variations for both R and QR signals in particular situations in Section 4. It is easy to verify from (1), (11), (13), (14), (17) and (18), that, for both R and QR signals, $z_{F_M}(m)$ can be written as

$$z_{F_M}(m) = b_m r_{m,m} + \sum_{\ell\neq m} b_\ell \text{Re}(r_{m,\ell}) + z_{n,F_M}(m), \tag{20}$$

where $z_{n,F_M}(m) = \text{Re}[y_{n,F_M}(m)]$ for R signals, $z_{n,F_M}(m) = \text{Re}[i^{-m}y_{n,F_M}(m)]$ for QR signals and where $y_{n,F_M}(m)$ is defined by (17) for $\ell=m$ with $\mathbf{n}_{F_M}(f)$ instead of $\mathbf{x}_{F_M}(f)$. The output SINR on the current symbol m is then defined by:

$$\overset{\text{def}}{=} \frac{\pi_b r^2_{m,m}}{\text{E}[z^2_{n,F_M}(m)]} = \frac{2\pi_b r^2_{m,m}}{\text{E}|y^2_{n,F_M}(m)| + \epsilon^2_{0,m}\text{Re}(\text{E}[y^2_{n,F_M}(m)])}. \tag{21}$$

[1] Note that this real part capture is useless for $M=2$ for R and QR signals, as it is proved in Appendix for QR signals.

In the presence of R or QR CCI and for a given value of m, the total noise, $y_{n,F_M,m}(t)$, at the output of the filter (19) for $\ell = m$, such that $y_{n,F_M,m}(mT) = y_{n,F_M}(m)$, is SO cyclostationary, which implies that $\mathrm{E}|y^2_{n,F_M}(m)|$ and $\mathrm{E}[y^2_{n,F_M}(m)]$ have Fourier series expansions given by Gardner [2]:

$$\mathrm{E}|y^2_{n,F_M}(m)| = \sum_{\gamma_k} e^{i2\pi\gamma_k mT} \int r^{\gamma_k}_{y_{n,F_M,m}}(f)df \tag{22}$$

$$\mathrm{E}[y^2_{n,F_M}(m)] = \sum_{\delta_k} e^{i2\pi\delta_k mT} \int c^{\delta_k}_{y_{n,F_M,m}}(f)df. \tag{23}$$

Here, the quantities γ_k and δ_k denote the non-conjugate and conjugate SO cyclic frequencies of $y_{n,F_M,m}(t)$, respectively, whereas $r^{\gamma_k}_{y_{n,F_M,m}}(f)$ and $c^{\delta_k}_{y_{n,F_M,m}}(f)$ are the Fourier transforms of the first, $r^{\gamma_k}_{y_{n,F_M,m}}(\tau)$, and second, $c^{\delta_k}_{y_{n,F_M,m}}(\tau)$, cyclic correlation functions of $y_{n,F_M,m}(t)$ for the delay τ and the cyclic frequencies γ_k and δ_k, respectively. Moreover, as $y_{n,F_M,m}(t)$ is the output of the filter (19) for $\ell = m$, whose input is $\mathbf{n}_{F_M}(t)$, we can write:

$$r^{\gamma_k}_{y_{n,F_M,m}}(f) = \mathbf{w}^H_{F_M,m}(f+\gamma_k/2)\mathbf{R}^{\gamma_k}_{n_{F_M}}(f)\mathbf{w}_{F_M,m}(f-\gamma_k/2) \tag{24}$$

$$c^{\delta_k}_{y_{n,F_M,m}}(f) = \mathbf{w}^H_{F_M,m}(f+\delta_k/2)\mathbf{C}^{\delta_k}_{n_{F_M}}(f)\mathbf{w}^*_{F_M,m}(\delta_k/2-f), \tag{25}$$

where $\mathbf{R}^{\gamma_k}_{n_{F_M}}(f)$ and $\mathbf{C}^{\delta_k}_{n_{F_M}}(f)$ are the Fourier transforms of the first, $\mathbf{R}^{\gamma_k}_{n_{F_M}}(\tau)$, and second, $\mathbf{C}^{\delta_k}_{n_{F_M}}(\tau)$, cyclic correlation matrices of $\mathbf{n}_{F_M}(t)$ for the delay τ and the cyclic frequency γ_k and δ_k, respectively. Using (18), (22) and (23) into (21), we obtain an alternative expression of (21) given by:

$$\mathrm{SINR}_{F_M}(m) = \frac{2\pi_b(\int \mathbf{g}^H_{F_M,m}(f)[\mathbf{R}^0_{n_{F_M}}(f)]^{-1}\mathbf{g}_{F_M,m}(f)df)^2}{\sum_{\gamma_k} e^{i2\pi\gamma_k mT}\int r^{\gamma_k}_{y_{n,F_M,m}}(f)df + \epsilon^2_{0,m}\mathrm{Re}[\sum_{\delta_k} e^{i2\pi\delta_k mT}\int c^{\delta_k}_{y_{n,F_M,m}}(f)df]}, \tag{26}$$

where $r^{\gamma_k}_{y_{n,F_M,m}}(f)$ and $c^{\delta_k}_{y_{n,F_M,m}}(f)$ are given by (24) and (25), respectively. Expressions (24) and (25) show that the non-conjugate and conjugate SO cyclic frequencies of the output $y_{n,F_M,m}(t)$ of the filter whose frequency response is $\mathbf{w}^H_{F_M,m}(f)$ are those of the input $\mathbf{n}_{FM}(t)$. Consequently, in the presence of a CCI having the same nature (R or QR) and symbol period as the SOI and a FO equal to Δ_f, the non-conjugate γ_k and conjugate δ_k SO cyclic frequencies of the output $y_{n,F_M,m}(t)$ of the filter $\mathbf{w}^H_{F_M,m}(f)$ are from (1), (6), (7), (11), (13) and (14), $\gamma_k = \alpha_k = k/T, k \in \mathbb{Z}$, for $M = 1, 2$ and R signals and for $M = 1, 2, 3$ and QR signals, $\delta_k = \beta_k = 2\Delta_f + k/T, k \in \mathbb{Z}$, for $M = 1, 2$ and R signals and $\delta_k = \beta_k = 2\Delta_f + (2k+1)/2T, k \in \mathbb{Z}$ for $M = 1, 2, 3$ and QR signals. Inserting these results into (26), we obtain a new expression of $\mathrm{SINR}_{F_M}(m)$, valid for $M = 1, 2$ and R signals and for $M = 1, 2, 3$ and QR signals and given by

$$\mathrm{SINR}_{F_M}(m) = \frac{2\pi_b(\int \mathbf{g}^H_{F_M,m}(f)[\mathbf{R}^0_{n_{F_M}}(f)]^{-1}\mathbf{g}_{F_M,m}(f)df)^2}{\sum_{\alpha_k}\int r^{\alpha_k}_{y_{n,F_M,m}}(f)df + \mathrm{Re}[\sum_{\beta_k} e^{i4\pi\Delta_f mT}\int c^{\beta_k}_{y_{n,F_M,m}}(f)df]}, \tag{27}$$

4. SINR analysis

4.1. Objectives and extended M-input total noise cyclic statistics

In this section, we analyze both analytically and by simulations, for $M = 1, 2$ and R signals and for $M = 1, 2, 3$ and QR signals, the impact on the output SINR at time mT, $\mathrm{SINR}_{F_M}(m)$, of the different parameters and of the CCI FO Δ_f in particular. The first purpose is to verify, for both R and QR signals, the effectiveness of the extended two-input WL FRESH receivers with respect to the conventional ones, in performing SAIC/MAIC for an arbitrary value of Δ_f. For values of Δ_f generating a spectrum overlapping between the SOI and the CCI, the second and third purposes are respectively to show the less efficiency of the extended two-input WL FRESH receiver for QR signals with respect to R ones and the improvement of performance obtained for QR signals with the extended three-input WL FRESH receiver. Finally, the fourth purpose is to analyze the relative role of both spectrum and phase discriminations as a function of Δ_f at the output of the extended two and three-input WL FRESH receivers, which has never been analyzed in the literature.

Considering the total noise model assumed in (1), we have followed the same approach as [38, Appendix A] and have proved that the matrices $\mathbf{R}^{\alpha_k}_{n_{F_M}}(f)$ and $\mathbf{C}^{\beta_k}_{n_{F_M}}(f)$ appearing in (27) through (24) and (25) can be written, for R signals and $M = 1, 2$, as

$$\mathbf{R}^{\alpha_k}_{n_{F_M}}(f) = (\pi_d/T)\mathbf{g}_{l_0,F_M}(f+\alpha_k/2)\mathbf{g}^H_{l_0,F_M}(f-\alpha_k/2) + N_0\delta(\alpha_k)\mathbf{I}_{MN}, \tag{28}$$

$$\begin{aligned}\mathbf{C}^{\beta_k}_{n_{F_M}}(f) = {} & (\pi_d/T)\mathbf{g}_{l_0,F_M}(f+\beta_k/2)\mathbf{g}^T_{l_0,F_M}(\beta_k/2-f) \\ & + N_0\delta(\beta_k - 2\Delta_f)\delta(M-2)\mathbf{J}\end{aligned} \tag{29}$$

and for QR signals and $M = 1, 2, 3$ as

$$\begin{aligned}\mathbf{R}^{\alpha_k}_{n_{F_M}}(f) = {} & (\pi_d/T)\mathbf{g}_{l_0,F_M}(f+\alpha_k/2)\mathbf{g}^H_{l_0,F_M}(f-\alpha_k/2) \\ & + N_0\delta(\alpha_k)\mathbf{I}_{MN} + N_0\delta(\alpha_k - 1/T)\delta(M-3)\mathbf{J}_1 \\ & + N_0\delta(\alpha_k + 1/T)\delta(M-3)\mathbf{J}^T_1,\end{aligned} \tag{30}$$

$$\begin{aligned}\mathbf{C}^{\beta_k}_{n_{F_M}}(f) = {} & (\pi_d/T)\mathbf{g}_{l_0,F_M}(f+\beta_k/2)\mathbf{g}^T_{l_0,F_M}(\beta_k/2-f) \\ & + N_0\delta(\beta_k - 2\Delta_f - 1/2T)\delta(M-2)\mathbf{J} \\ & + N_0\delta(\beta_k - 2\Delta_f - 1/2T)\delta(M-3)\mathbf{J}_2 \\ & + N_0\delta(\beta_k - 2\Delta_f + 1/2T)\delta(M-3)\mathbf{J}_3.\end{aligned} \tag{31}$$

Here, $\mathbf{g}_{l_0,F_1}(f) \overset{\text{def}}{=} \mathbf{g}_{l_0}(f)$ for both R and QR signals, $\mathbf{g}_{l_0,F_2}(f) \overset{\text{def}}{=} [\mathbf{g}^T_{l_0}(f), \mathbf{g}^H_{l_0}(2\Delta_f - f)]^T$ for R signals, $\mathbf{g}_{l_0,F_2}(f) \overset{\text{def}}{=} [\mathbf{g}^T_{l_0}(f), \mathbf{g}^H_{l_0}(2\Delta_f + 1/2T - f)]^T$ and $\mathbf{g}_{l_0,F_3}(f) \overset{\text{def}}{=} [\mathbf{g}^T_{l_0}(f), \mathbf{g}^H_{l_0}(2\Delta_f + 1/2T - f), \mathbf{g}^H_{l_0}(2\Delta_f - 1/2T - f)]^T$ for QR signals, $\pi_d \overset{\text{def}}{=} \mathrm{E}(d^2_\ell)$, N_0 is the power spectral density of each component of the background noise $\mathbf{u}(t)$, $\mathbf{J}$ is the $2N \times 2N$ matrix and $\mathbf{J}_1$, $\mathbf{J}_2$ and $\mathbf{J}_3$ are the $3N \times 3N$ matrices defined by

$$\mathbf{J} = \begin{pmatrix}\mathbf{0} & \mathbf{I}\\ \mathbf{I} & \mathbf{0}\end{pmatrix},\ \mathbf{J}_1 = \begin{pmatrix}\mathbf{0} & \mathbf{0} & \mathbf{0}\\ \mathbf{0} & \mathbf{0} & \mathbf{I}\\ \mathbf{0} & \mathbf{0} & \mathbf{0}\end{pmatrix},\ \mathbf{J}_2 = \begin{pmatrix}\mathbf{0} & \mathbf{I} & \mathbf{0}\\ \mathbf{I} & \mathbf{0} & \mathbf{0}\\ \mathbf{0} & \mathbf{0} & \mathbf{0}\end{pmatrix} \text{ and}$$

$$\mathbf{J}_3 = \begin{pmatrix}\mathbf{0} & \mathbf{0} & \mathbf{I}\\ \mathbf{0} & \mathbf{0} & \mathbf{0}\\ \mathbf{I} & \mathbf{0} & \mathbf{0}\end{pmatrix}. \tag{32}$$

4.2. SINR computation and analysis for channels with no delay spread

4.2.1. Propagation channel model

To get more insights into the comparative behaviour of the extended M-input pseudo-MLSE receivers for R ($M = 1, 2$) and QR ($M = 1, 2, 3$) signals, we assume in this Section 4.2 a square root raised cosine (SRRC) pulse shaping filter (1/2 Nyquist filter) $v(t)$ with a roll off ω. The SOI and CCI have the same bandwidth $B = (1+\omega)/T$, and spectrally overlap if $0 \le |\Delta_f|T \le (1+\omega)$, as illustrated in Fig. 2, what we assume in the following.

The SAIC/MAIC extension developed in the previous sections for a CCI with a non-zero FO has been done for arbitrary frequency

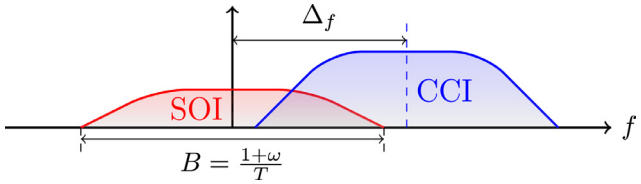

Fig. 2. Spectral representation of the SOI and CCI.

selective propagation channels. However, to easily describe the behaviour and quantify the performance of the generic extended M-input pseudo-MLSE receivers from interpretable analytic expressions of $\mathrm{SINR}_{F_M}(m)$ defined by (27), we must restrict the analysis in this Section 4.2 to propagation channels with no delay spread such that

$$\mathbf{h}(t) = \mu\delta(t)\mathbf{h} \quad \text{and} \quad \mathbf{h}_I(t) = \mu_I\delta(t-\tau_I)\mathbf{h}_I. \tag{33}$$

Here μ and μ_I control the amplitude of the SOI and CCI respectively and τ_I is the delay of the CCI with respect to the SOI. The vectors $\mathbf{h}$ and $\mathbf{h}_I$, random or deterministic, with components $h(k)$ and $h_I(k)$, $1 \le k \le N$, respectively and such that $\mathrm{E}(|h(k)|^2) = \mathrm{E}(|h_I(k)|^2) = 1$, correspond to the channel vectors of the SOI and CCI, respectively. The mean powers of the SOI and CCI at the output of each antenna are given by $P_s \overset{\text{def}}{=} <\mathrm{E}(|\mu s(t)h(k)|^2)> = \mu^2\pi_b/T$ and $P_j \overset{\text{def}}{=} <\mathrm{E}(|\mu_I j(t)h_I(k)|^2)> = \mu_I^2\pi_d/T$ respectively, where $j(t)$ is defined by (8) with c_ℓ instead of a_ℓ.

4.2.2. Deterministic channels and zero roll-off

Under the previous assumptions, analytical interpretable expressions of $\mathrm{SINR}_{F_M}(m)$ defined by (27) are only possible for a zero roll-off ω, which is assumed in this subsection. Otherwise, the computation of (27) can only be done numerically by computer simulations and will be discussed in the following subsection. For a zero roll-off, the quantities $\pi_s \overset{\text{def}}{=} \mu^2\pi_b$, $\pi_I \overset{\text{def}}{=} \mu_I^2\pi_d$ and N_0 correspond to the mean power of the SOI, the CCI (for $\Delta_f = 0$) and the background noise per antenna at the output of the pulse shaping matched filter respectively. We then denote by ϵ_s and ϵ_I the quantities $\epsilon_s \overset{\text{def}}{=} \pi_s\|\mathbf{h}\|^2/N_0$ and $\epsilon_I \overset{\text{def}}{=} \pi_I\|\mathbf{h}_I\|^2/N_0$ and by $\mathrm{SINR}_{R_M}(m)$ and $\mathrm{SINR}_{QR_M}(m)$ the SINR (27) at the output of the extended M-input pseudo-MLSE receiver for R and QR signals respectively. Moreover, we assume in this subsection deterministic channels and we denote by $\alpha_{s,I}$ the spatial correlation coefficient between the SOI and the CCI, such that $(0 \le |\alpha_{s,I}| \le 1)$, and defined by

$$\alpha_{s,I} \overset{\text{def}}{=} \frac{\mathbf{h}^H\mathbf{h}_I}{\|\mathbf{h}\|\|\mathbf{h}_I\|} \overset{\text{def}}{=} |\alpha_{s,I}|e^{i\phi_{s,I}} \tag{34}$$

Using (19), (27), (28) to (31), (33), (34), we obtain, the following expressions proved in Appendix:

$$\mathrm{SINR}_{R_1}(m) = \frac{2\epsilon_s}{1+2\epsilon_I\cos^2\phi_{s,I}}, (|\alpha_{s,I}|, \Delta_f) = (1,0), \tag{35}$$

$$\mathrm{SINR}_{QR_1}(m) = \frac{2\epsilon_s}{1+\epsilon_I\left[1+\cos(2\phi_{s,I})\cos\frac{\pi\tau_I}{T}\right]}, (|\alpha_{s,I}|, \Delta_f) = (1,0), \tag{36}$$

$$\mathrm{SINR}_{R_2}(m) = \frac{2\epsilon_s}{1+2\epsilon_I}, (|\alpha_{s,I}|, \Delta_f, \psi_{s,I,m}) = (1,0,k\pi), \tag{37}$$

$$\mathrm{SINR}_{QR_2}(m) = \frac{9\epsilon_s}{2\epsilon_I}\frac{1}{[3+2\cos 4\phi_{s,I}]}, (|\alpha_{s,I}|, \Delta_f, \kappa_{s,I,m}) = (1,0,k\pi), \tag{38}$$

$$\mathrm{SINR}_{QR_3}(m) = \frac{\epsilon_s}{\epsilon_I}, (|\alpha_{s,I}|, \Delta_f, \kappa_{s,I,m}, \zeta_{s,I,m}) = (1,0,k\pi,k'\pi), \tag{39}$$

whereas, assuming a strong CCI ($\epsilon_I \gg 1$), we obtain

$$\begin{aligned}\mathrm{SINR}_{R_1}(m) &\approx \mathrm{SINR}_{QR_1}(m)\\ &\approx 2\epsilon_s[1-|\alpha_{s,I}^2|(1-|\Delta_f|T)], (|\alpha_{s,I}|, \Delta_f) \ne (1,0),\end{aligned} \tag{40}$$

$$\mathrm{SINR}_{R_2}(m) \approx 2\epsilon_s\left[1-\frac{|\alpha_{s,I}^2|}{2}(1-|\Delta_f|T)\right], 0.5 \le |\Delta_f|T \le 1, \tag{41}$$

$$\begin{aligned}\mathrm{SINR}_{R_2}(m) \approx 2\epsilon_s\left[1-|\alpha_{s,I}^2|\left\{\frac{|\Delta_f|T}{2}+(1-2|\Delta_f|T])\cos^2\psi_{s,I,m}\right\}\right],\\ |\Delta_f|T \le 0.5, (|\alpha_{s,I}|, \Delta_f, \psi_{s,I,m}) \ne (1,0,k\pi),\end{aligned} \tag{42}$$

$$\mathrm{SINR}_{QR_2}(m) \approx 2\epsilon_s[1-|\alpha_{s,I}^2|(1-|\Delta_f|T)], 0.5 \le |\Delta_f|T \le 1, \tag{43}$$

$$\mathrm{SINR}_{QR_2}(m) \approx 2\epsilon_s\left[1-\frac{|\alpha_{s,I}^2|}{2}\left(\frac{3}{2}-|\Delta_f|T\right)\right], 0.25 \le |\Delta_f|T \le 0.5, \tag{44}$$

$$\begin{aligned}\mathrm{SINR}_{QR_2}(m) \approx 2\epsilon_s\left[1-\frac{|\alpha_{s,I}^2|}{2}\left(1+|\Delta_f|T+(1-4|\Delta_f|T)\cos^2\kappa_{s,I,m}\right)\right],\\ |\Delta_f|T \le 0.25, (|\alpha_{s,I}|, \Delta_f, \kappa_{s,I,m}) \ne (1,0,k\pi),\end{aligned} \tag{45}$$

$$\begin{aligned}\mathrm{SINR}_{QR_3}(m) \approx 2\epsilon_s\left[1-|\alpha_{s,I}^2|\frac{(p_{1,m}+p_{2,m}|\Delta_f|T)-|\alpha_{s,I}^2|(p_{3,m}+p_{4,m}|\Delta_f|T)^2}{9-|\alpha_{s,I}^2|(p_{5,m}+p_{6,m}|\Delta_f|T)}\right],\\ (|\alpha_{s,I}|, \Delta_f, \kappa_{s,I,m}, \zeta_{s,I,m}) \ne (1,0,k\pi,k'\pi),\end{aligned} \tag{46}$$

where, similarly to $\mathrm{SINR}_{QR_2}(m)$, $\mathrm{SINR}_{QR_3}(m)$ is a continuous function of $|\Delta_f|T$ such that

$$\begin{aligned}p_{1,m}+p_{2,m}|\Delta_f|T &= 5(1-|\Delta_f|T)\\ p_{3,m}+p_{4,m}|\Delta_f|T &= 2(1-|\Delta_f|T)\\ p_{5,m}+p_{6,m}|\Delta_f|T &= 7(1-|\Delta_f|T), 0.75 \le |\Delta_f|T \le 1\end{aligned} \tag{47}$$

$$\begin{aligned}p_{1,m}+p_{2,m}|\Delta_f|T &= -1+12\cos^2\zeta_{s,I,m}+|\Delta_f|T\left(3-16\cos^2\zeta_{s,I,m}\right)\\ p_{3,m}+p_{4,m}|\Delta_f|T &= 0.5+3\cos^2\zeta_{s,I,m}-4|\Delta_f|T\cos^2\zeta_{s,I,m}\\ p_{5,m}+p_{6,m}|\Delta_f|T &= 4+6\cos^2\zeta_{s,I,m}-|\Delta_f|T\left(3+8\cos^2\zeta_{s,I,m}\right), 0.5\\ &\le |\Delta_f|T \le 0.75\end{aligned} \tag{48}$$

$$\begin{aligned}p_{1,m}+p_{2,m}\left|\Delta_f\right|T &= 3+4\cos^2\zeta_{s,I,m}-5\left|\Delta_f\right|T\\ p_{3,m}+p_{4,m}\left|\Delta_f\right|T &= 1.5+\cos^2\zeta_{s,I,m}-2\left|\Delta_f\right|T\\ p_{5,m}+p_{6,m}\left|\Delta_f\right|T &= 6+2\cos^2\zeta_{s,I,m}-7\left|\Delta_f\right|T,\\ &0.25 \le |\Delta_f|T \le 0.5\end{aligned} \tag{49}$$

$$\begin{aligned}p_{1,m}+p_{2,m}\left|\Delta_f\right|T &= 1+4\cos^2\kappa_{s,I,m}+4\cos^2\zeta_{s,I,m}\\ &\quad +|\Delta_f|T\left(3-16\cos^2\kappa_{s,I,m}\right)\\ p_{3,m}+p_{4,m}\left|\Delta_f\right|T &= 1+\cos^2\kappa_{s,I,m}+\cos^2\zeta_{s,I,m}-4\left|\Delta_f\right|T\cos^2\kappa_{s,I,m}\\ p_{5,m}+p_{6,m}\left|\Delta_f\right|T &= 5+2\cos^2\kappa_{s,I,m}+2\cos^2\zeta_{s,I,m}\\ &\quad -|\Delta_f|T\left(3+8\cos^2\kappa_{s,I,m}\right),\\ &\quad |\Delta_f|T \le 0.25\end{aligned} \tag{50}$$

and where $\psi_{s,I,m}$, $\kappa_{s,I,m}$ and $\zeta_{s,I,m}$ are defined by

$$\psi_{s,I,m} \quad \phi_{s,I}+2\pi\Delta_f(mT-\tau_I) \tag{51}$$

$$\kappa_{s,I,m} \quad \phi_{s,I} + 2\pi\,\Delta_f(mT - \tau_I) - \pi\,\tau_I/2T \tag{52}$$

$$\zeta_{s,I,m} \quad \phi_{s,I} + 2\pi\,\Delta_f(mT - \tau_I) + \pi\,\tau_I/2T. \tag{53}$$

Note that most of expressions (39) to (50) are completely new and have never been presented elsewhere. Let us recall that a receiver performs MAIC (for $N > 1$) or SAIC (for $N = 1$), at time mT, as $\epsilon_I \to \infty$ if the associated $\mathrm{SINR}_{F_M}(m)$ does not converge toward zero.

We deduce from (35) (36) and (40) that, for both R and QR signals and for a strong CCI, the conventional receiver ($M = 1$) performs MAIC as soon as $|\alpha_{s,I}| \neq 1$, i.e., when there is a spatial discrimination between the sources, and performs SAIC as long as $\Delta_f \neq 0$, i.e., when there is a spectral discrimination between the sources. In these two latter cases, the conventional receiver is not sensitive to the phase of the signals and the output SINR does not depend on m. The SINR is maximum and equal to $2\epsilon_s$, the one obtained without CCI, if the sources are either spatially orthogonal ($\alpha_{s,I} = 0$) or do not spectrally overlap ($|\Delta_f|T = 1$). Otherwise, the output SINR decreases as $|\alpha_{s,I}|$ increases, i.e., as the spatial discrimination between the sources decreases, and as $|\Delta_f|T$ decreases, i.e., as the spectral overlap between the sources increases. For $N = 1$, we have $|\alpha_{s,I}| = 1$ and (40) becomes $\mathrm{SINR}_{R_1} \approx \mathrm{SINR}_{QR_1} \approx 2\epsilon_s\Delta_f T$, which shows that the SINR strongly decreases as the overlap between the sources strongly increases. For a complete overlap ($\Delta_f = 0$), (35) and (36) show that SAIC of a strong CCI at the output of the conventional receiver is generally no longer possible, except when $\phi_{s,I} = (2k+1)\pi/2$ for R signals and $(\tau_I/T, \phi_{s,I}) = (2k_1, (2k_2+1)\pi/2)$ or $(\tau_I/T, \phi_{s,I}) = (2k_1+1, k_2\pi)$ for QR signals, where k, k_1 and k_2 are integers.

Moreover, we deduce from (41) to (45) that, for both R and QR signals and a strong CCI, the extended two-input pseudo-MLSE receiver performs MAIC as soon as $|\alpha_{s,I}| \neq 1$. Besides, we deduce from (41), (43) and (44) that for a strong CCI and a spectral overlap which is less that 50% for R signals and less that 75% for QR signals, the extended two-input pseudo-MLSE receiver is not sensitive to the phase of the signals and discriminates the sources only spatially and spectrally. In this case, the output SINR does not depend on m. For $N = 1$ and under the previous assumptions, the extended two-input receiver performs SAIC thanks to a spectral discrimination between the sources only. Nevertheless, while its performance correspond to those of the conventional receiver for a QR CCI whose spectral overlap with the SOI is less than 50%, it has better performance than the conventional receiver for a spectral overlap which is less than 50% for a R CCI and which is comprised between 50% and 75% for a QR CCI. This proves, in this case, the great interest of the extended two-input pseudo-MLSE receiver for both R and QR signals and the better performance obtained for R signals with respect to QR signals at least for a spectral overlap lower than 50%.

On the other hand, (42), (45), (51) and (52) show that for a strong CCI and a spectral overlap which is greater than 50% for R signals and greater than 75% for QR signals, the extended two-input pseudo-MLSE receiver discriminates the sources spatially, spectrally and by phase and the output SINR depends on the differential phase of the sources and on the symbol time mT. It completely cancels the CCI as long as there is at least one of the three discriminations between the sources, i.e., as long as $(|\alpha_{s,I}|, \Delta_f, \psi_{s,I,m}) \neq (1, 0, k\pi)$ for R signals and $(|\alpha_{s,I}|, \Delta_f, \kappa_{s,I,m}) \neq (1, 0, k\pi)$ for QR signals. For $N = 1$ and under the previous assumptions, the extended two-input pseudo-MLSE receiver performs SAIC as long as there is a spectral ($\Delta_f \neq 0$) or a phase ($\psi_{s,I,m} \neq 0$ for R signals and $\kappa_{s,I,m} \neq 0$ for QR signals) discrimination between the sources. However, as long as the spatial discrimination between the sources is not total ($\alpha_{s,I} \neq 0$), (42) and (45) show that the relative weight of the phase discrimination with respect to the spectral one increases with the overlap for both R and QR signals. In other words, the phase discrimination takes over from the spectral one when the latter becomes too weak, which generates better performance than the conventional receiver for both MAIC and SAIC. In particular, for a complete overlap ($\Delta_f = 0$), (42) and (45) reduce respectively to

$$\mathrm{SINR}_{R_2} \approx 2\epsilon_s(1 - |\alpha_{s,I}^2|\cos^2\phi_{s,I}),\ (|\alpha_{s,I}|, \phi_{s,I}) \neq (1, k\pi) \tag{54}$$

$$\mathrm{SINR}_{QR_2} \approx 2\epsilon_s\left[1 - \frac{|\alpha_{s,I}^2|}{2}(1 + \cos^2\kappa_{s,I})\right],\ (|\alpha_{s,I}|, \kappa_{s,I}) \neq (1, k\pi), \tag{55}$$

where $\kappa_{s,I} \overset{\text{def}}{=} \phi_{s,I} - \pi\,\tau_I/2T$, which have been obtained in Chevalier et al. [38] and which only depend on the differential phase of the sources for $N = 1$. All these results enlighten, for arbitrary values of Δ_f, the great interest of the extended two-input pseudo MLSE receiver with respect to the conventional one for both R and QR signals. However, despite similar models (1) and (12) for R and QR signals, respectively, and similar processing (19), (41) to (45) show that the output SINRs for R and QR signals correspond to different expressions. This proves the non equivalence of R and derotated QR signals, for arbitrary values of Δ_f, for the efficient extended two-input filtering (19) in the presence of CCI, result which extends to arbitrary values of Δ_f, the one obtained in Chevalier et al. [38] for $\Delta_f = 0$.

To go further into the comparison of $\mathrm{SINR}_{R_2}(m)$ and $\mathrm{SINR}_{QR_2}(m)$ for a zero roll-off ($\omega = 0$) and a strong CCI ($\epsilon_I \gg 1$), whatever the value of $\phi_{s,I}$, τ_I and m, we must consider a statistical perspective. More precisely, for given values of T, $\Delta_f \neq 0$, τ_I and m, we now assume that $\phi_{s,I}$ is a random variable uniformly distributed on $[0, 2\pi]$. Under this assumption, we easily deduce from (40) to (45) the expectation of the output SINRs given by

$$\begin{aligned}\mathrm{E}[\mathrm{SINR}_{R_1}(m)] &\approx \mathrm{E}[\mathrm{SINR}_{QR_1}(m)] \\ &\approx 2\epsilon_s[1 - |\alpha_{s,I}^2|(1 - |\Delta_f|T)],\ (|\alpha_{s,I}|, \Delta_f) \neq (1, 0),\end{aligned} \tag{56}$$

$$\mathrm{E}[\mathrm{SINR}_{R_2}(m)] \approx 2\epsilon_s\left[1 - \frac{|\alpha_{s,I}^2|}{2}(1 - |\Delta_f|T)\right],\ |\Delta_f|T \leq 1, \tag{57}$$

$$\mathrm{E}[\mathrm{SINR}_{QR_2}(m)] \approx 2\epsilon_s\left[1 - \frac{|\alpha_{s,I}^2|}{2}\left(\frac{3}{2} - |\Delta_f|T\right)\right],\ |\Delta_f|T \leq 0.5, \tag{58}$$

$$\mathrm{E}[\mathrm{SINR}_{QR_2}(m)] \approx 2\epsilon_s[1 - |\alpha_{s,I}^2|(1 - |\Delta_f|T)],\ 0.5 \leq |\Delta_f|T \leq 1, \tag{59}$$

which reduce, for $|\alpha_{s,I}| = 1$, which includes the case $N = 1$, to

$$\mathrm{E}[\mathrm{SINR}_{R_1}(m)] \approx \mathrm{E}[\mathrm{SINR}_{QR_1}(m)] \approx 2\epsilon_s|\Delta_f|T,\ |\Delta_f|T \leq 1, \tag{60}$$

$$\mathrm{E}[\mathrm{SINR}_{R_2}(m)] \approx \epsilon_s(1 + |\Delta_f|T),\ |\Delta_f|T \leq 1, \tag{61}$$

$$\mathrm{E}[\mathrm{SINR}_{QR_2}(m)] \approx \epsilon_s(0.5 + |\Delta_f|T),\ |\Delta_f|T \leq 0.5, \tag{62}$$

$$\mathrm{E}[\mathrm{SINR}_{QR_2}(m)] \approx 2\epsilon_s|\Delta_f|T,\ 0.5 \leq |\Delta_f|T \leq 1. \tag{63}$$

These expressions show that if the sources are either spatially orthogonal ($\alpha_{s,I} = 0$) or do not spectrally overlap ($|\Delta_f|T = 1$), $\mathrm{E}[\mathrm{SINR}_{R_1}(m)] = \mathrm{E}[\mathrm{SINR}_{QR_1}(m)] = \mathrm{E}[\mathrm{SINR}_{R_2}(m)] = \mathrm{E}[\mathrm{SINR}_{QR_2}(m)] = 2\epsilon_s$ and the conventional and two-input receiver are equivalent and optimal for both R and QR signals. Otherwise, i.e., when $\alpha_{s,I} \neq 0$ and $|\Delta_f|T \neq 1$, (56) to (63) show that $\mathrm{E}[\mathrm{SINR}_{R_1}(m)] =$

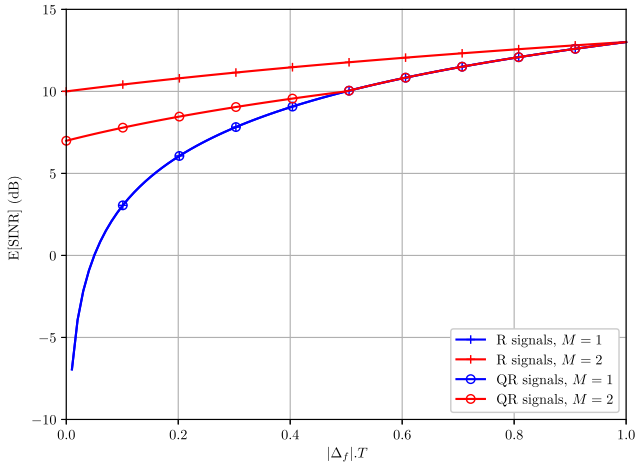

Fig. 3. $\mathrm{E}[\mathrm{SINR}_{R_M}]$ and $\mathrm{E}[\mathrm{SINR}_{QR_M}]$ $(M = 1, 2)$ as a function of $|\Delta_f|T$ for $\omega = 0$, $N = 1$, $\epsilon_s = 10$ dB, $\epsilon_I = 20$ dB, deterministic one tap channels.

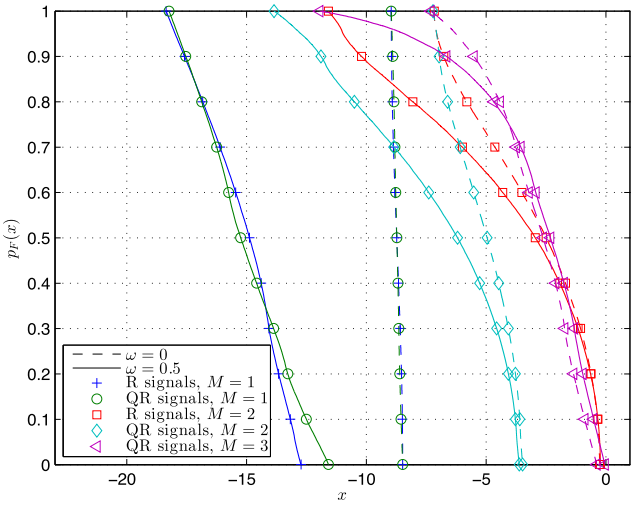

Fig. 4. $p_F(x)$ as a function of x for $N = 1$, $\epsilon_s = 10$ dB, $\epsilon_I = 20$ dB, ω=0, 0.5, deterministic one tap channels, R and QR signals, $|\Delta_f|T$=0.125.

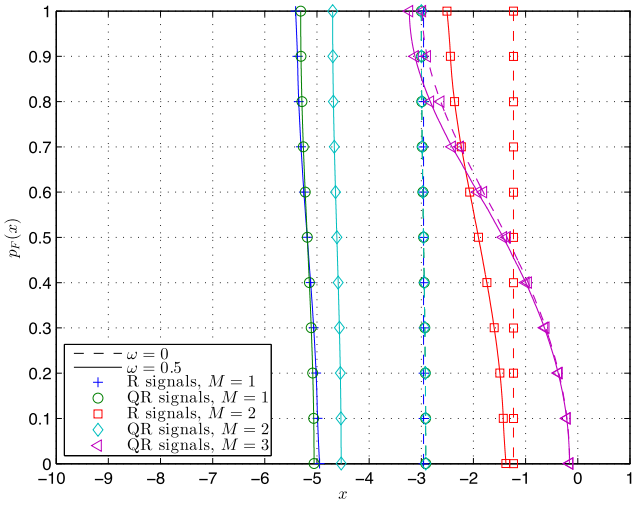

Fig. 5. $p_F(x)$ as a function of x for $N = 1$, $\epsilon_s = 10$ dB, $\epsilon_I = 20$ dB, ω=0, 0.5, deterministic one tap channels, R and QR signals, $|\Delta_f|T$=0.50.

$\mathrm{E}[\mathrm{SINR}_{QR_1}(m)] \leq \mathrm{E}[\mathrm{SINR}_{QR_2}(m)] < \mathrm{E}[\mathrm{SINR}_{R_2}(m)]$, which definitely proves, at least for a zero roll-off, that QR signals are less efficient than R ones for the extended two-input receiver (19) in the presence of one strong CCI with an arbitrary FO Δ_f, result which extends the one obtained in Chevalier et al. [38] for $\Delta_f = 0$. Besides, for $|\alpha_{s,I}| = 1$, as the overlap increases toward 100%, $\mathrm{E}[\mathrm{SINR}_{R_1}(m)] \approx \mathrm{E}[\mathrm{SINR}_{QR_1}(m)]$ decreases toward zero, while $\mathrm{E}[\mathrm{SINR}_{QR_2}(m)]$ and $\mathrm{E}[\mathrm{SINR}_{R_2}(m)]$ decreases toward $\epsilon_s/2$ and ϵ_s, respectively. This shows, for both R and QR signals, relatively stable mean performance of the two-input receiver whatever the overlap, contrary to that of the conventional receiver. Note that, to our knowledge, such an analysis from analytical SINR results at the output of a WL FRESH receiver for a CCI with FO have never been reported elsewhere. All the previous results are illustrated in Fig. 3 which shows the variations of $\mathrm{E}[\mathrm{SINR}_{R_M}]$ and $\mathrm{E}[\mathrm{SINR}_{QR_M}]$ $(M = 1, 2)$ as a function of $|\Delta_f|T$ for $N = 1$, $\epsilon_s = 10$ dB and $\epsilon_I = 20$ dB.

Finally, we deduce from (46) to (53) that, the SINR at the output of the three-input pseudo-MLSE receiver for QR signals is also maximum and equal to $2\epsilon_s$ if the sources are either spatially orthogonal ($\alpha_{s,I} = 0$) or do not spectrally overlap ($|\Delta_f|T = 1$). Otherwise, i.e., when $\alpha_{s,I} \neq 0$ and $|\Delta_f|T \neq 1$, the analytical analysis of (46) from (47) to (53) is complicated, even from a statistical perspective, except for $|\alpha_{s,I}| = 1$ and $0.75 \leq |\Delta_f|T \leq 1$ for which

$$\mathrm{SINR}_{QR_3}(m) \approx 2\epsilon_s \frac{(1 + 2|\Delta_f|T)^2}{2 + 7|\Delta_f|T}. \tag{64}$$

In this case, comparing (64) to (41) and (43), we deduce that $\mathrm{SINR}_{R_2}(m) \geq \mathrm{SINR}_{QR_3}(m) \geq \mathrm{SINR}_{QR_2}(m)$, which proves that the extended three-input pseudo-MLSE receiver improves the extended two-input one for QR signals. Otherwise, $\mathrm{SINR}_{QR_3}(m)$ must be analyzed from computer simulations, which is done in the next section.

4.2.3. Deterministic channels and arbitrary roll-off

To compare the performance of the three-input pseudo-MLSE receiver for QR signals to those of the two-input receiver for R and QR signals and to extend the results of the previous section to arbitrary values of the roll-off ω, we assume that $\phi_{s,I}$, $\pi\tau_I/2T$ and m (for $|\Delta_f| \neq 0$) are independent random variables uniformly distributed on $[0, 2\pi]$, $[0, 2\pi]$ and $\{0, 1, \ldots, 1/\lfloor|\Delta_f|T\rfloor\}$. Under these assumptions, choosing $\epsilon_s = 10$ dB and $\epsilon_I = 20$ dB, Figs. 4 and 5 show, for $|\Delta_f|T = 0.125$ and $|\Delta_f|T = 0.50$, respectively, for R and QR signals, for $N = 1$, $M = 1, 2$ for R signals and $M = 1, 2, 3$ for QR signals and for $\omega = 0,\ 0.5$, the variations of $\Pr[(\mathrm{SINR}_{F_M}(m)/2\epsilon_s)\mathrm{dB} \geq x\mathrm{dB}] \overset{\mathrm{def}}{=} p_{F_M}(x)$ as a function of x (dB), where Pr[.] means Probability. Note that the curves appearing in this figure are built from Monte-Carlo simulations where the $\mathrm{SINR}_{F_M}(m)$ has been computed from the general expression (27). Note the much better performance of the extended two-input receiver with respect to the conventional one for R signals for $(\omega, |\Delta_f|T) = (0, 0.5)$ and for both R and QR signals for $(\omega, |\Delta_f|T) \neq (0, 0.5)$, hence the interest of the extended two-input receiver in these cases.

Note the much better performance of the extended two-input receiver with respect to the conventional one for R signals for $(\omega, |\Delta_f|T) = (0, 0.5)$ and for both R and QR signals for $(\omega, |\Delta_f|T) \neq (0, 0.5)$, hence the interest of the extended two-input receiver in these cases. Note also, whatever ω and $|\Delta_f|T$, the lower performance obtained for QR signals with respect to R ones at the output of the extended two-input receiver and, for QR signals, the better performance obtained with $M = 3$ instead of $M = 2$, enlightening the great interest of the extended three-input receiver, i.e., of (14) with respect to (13). Note also, for both R and QR signals and for a given value of M, increasing performance with $|\Delta_f|T$ of the extended M-input WL FRESH receiver. For example, for $\omega = 0.5$ and $x = -5$ dB, we note, for $|\Delta_f|T = 0.125$, that $p_{QR_1}(x) = p_{R_1}(x) = 0\%$, $p_{QR_2}(x) \approx 37\%$, $p_{R_2}(x) \approx 64\%$, and $p_{QR_3}(x) \approx 82\%$, whereas for $|\Delta_f|T = 0.50$, we obtain $p_{QR_2}(x) = 37\%$ for $x \approx -4.6$ dB, $p_{R_2}(x) =$

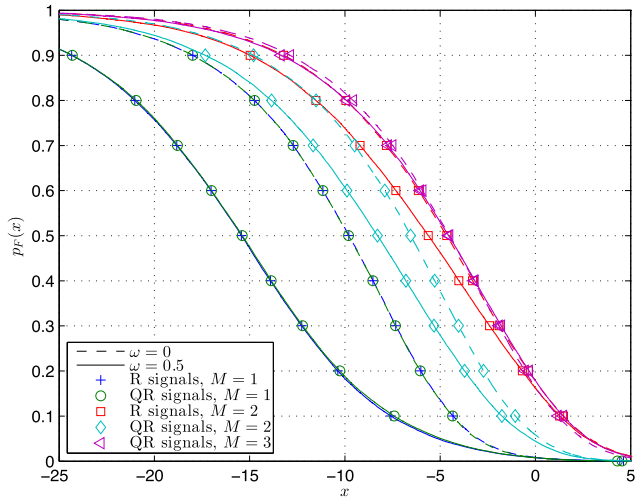

Fig. 6. $p_F(x)$ as a function of x for $N = 1$, $\epsilon_s = 10$ dB, $\epsilon_I = 20$ dB, $\omega = 0,\ 0.5$, Rayleigh one tap channels, R and QR signals, $|\Delta_f|T = 0.125$.

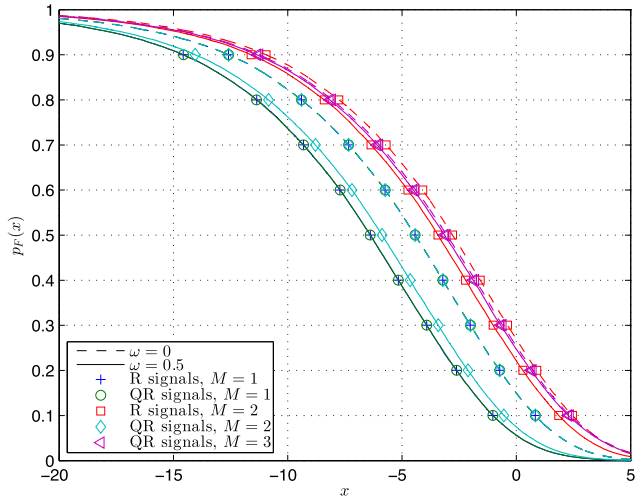

Fig. 7. $p_F(x)$ as a function of x for $N = 1$, $\epsilon_s = 10$ dB, $\epsilon_I = 20$ dB, $\omega = 0,\ 0.5$, Rayleigh one tap channels, R and QR signals, $|\Delta_f|T = 0.50$.

64% for $x \approx -2.1$ dB, and $p_{QR_3}(x) = 82\%$ for $x \approx -2.9$ dB, illustrating the previous results.

4.2.4. Random channels and arbitrary roll-off

The analysis done in Section 4.2.3 for arbitrary values of the roll-off ω is applied in this subsection, and under the same assumptions, to Rayleigh fading channels instead of deterministic channels and for R and QR signals. In this case, each component of $\mathbf{h}$ and $\mathbf{h}_I$ are i.i.d. random variables and follows a circular complex Gaussian distribution such that $\epsilon_s \overset{\text{def}}{=} \pi_s \mathrm{E}[\|\mathbf{h}\|^2]/\eta_2 = N\pi_s/\eta_2$ and $\epsilon_I \overset{\text{def}}{=} \pi_I \mathrm{E}[\|\mathbf{h}_I\|^2]/\eta_2 = N\pi_I/\eta_2$. Under these assumptions, Figs. 6 and 7 show the same variations as Figs. 4 and 5, respectively but for Rayleigh fading channels.

Again these figures show, for the two values of both $|\Delta_f|T$ and ω which have been considered, the better performance of the two-input receiver with respect to the conventional one for both R and QR signals, the lower performance obtained for QR signals with respect to R signals for $M = 2$ and the better performance obtained, for QR signals, with $M = 3$ with respect to $M = 2$. We still note for both R and QR signals and for a given value of M, the increasing performance of the extended M-input receiver with $|\Delta_f|T$.

5. Output SER of the extended pseudo-MLSE receivers for one CCI

We verify in this section that, in the presence of one CCI, the results obtained in Section 4 through the output SINR criterion are still valid for the output symbol error rate (SER) criterion. To this aim, we present some comparative performance in terms of output SER.

5.1. One tap deterministic channels

To compare the M-input ($M = 1, 2$) extended pseudo-MLSE receivers for R signals and the M-input ($M = 1, 2, 3$) extended pseudo-MLSE receivers for QR signals, from a SER criterion, we consider the transmission of 1000 frames of 184 symbols and we assume, in this subsection, one tap deterministic channels which are constant over a frame and random from a frame to another. For each frame, we assume that $\phi_{s,I}$ and $\tau_I/2T$ are independent random variables uniformly distributed on $[0, 2]$. Under these assumptions, Figs 8a, 8b and 8c show, for different values of $|\Delta_f|T$, the variations of the SER at the output of the considered receivers for both R and QR signals, as a function of ϵ_s, for $N = 1$, $\omega = 0.5$ and $\epsilon_I/\epsilon_s = 10$ dB. For these figures, $|\Delta_f|T = 0$ (a), 0.5 (b) and 1 (c). Note the increasing performance with $|\Delta_f|T$ of all the receivers. Note in particular the relatively poor performance of the conventional receivers ($M = 1$) for $|\Delta_f|T = 0$ and $|\Delta_f|T = 0.5$ and the much better performance of the M-input receivers for $M > 1$. Note also the better performance obtained with $M = 2$ for R signals with respect to QR signals. Note finally, for QR signals, the better performance obtained for $M = 3$ instead of $M = 2$.

5.2. One tap Rayleigh channels

To complete the previous results and under the assumptions of Figs. 8 and 9 shows, for $|\Delta_f|T = 0.5$ and 1, the same variations as Fig. 8, as a function of ϵ_s for Rayleigh fading channels for which $\mathbf{h}$ and $\mathbf{h}_I$ are circular Gaussian channels, such that $\epsilon_I/\epsilon_s = 10$ dB. The conclusions of Fig. 8 hold for Fig. 9.

5.3. Two tap deterministic channels

Finally, we consider in this subsection a one-tap deterministic channel for the SOI and a two-tap frequency selective deterministic channel for the CCI such that

$$\mathbf{h}(t) = \mu\delta(t)\mathbf{h} \quad \text{and} \quad \mathbf{h}_I(t) = \mu_{I_1}\delta(t - \tau_{I_1})\mathbf{h}_{I_1} + \mu_{I_2}\delta(t - \tau_{I_1} - T)\mathbf{h}_{I_2}, \tag{65}$$

where μ_{I_1} and μ_{I_2} control the amplitudes of the first and second paths of the CCI, whereas $\mathbf{h}_{I_1}$ and $\mathbf{h}_{I_2}$ correspond to the channel vectors of the latter, such that $\|\mathbf{h}_{I_1}\|^2 = \|\mathbf{h}_{I_2}\|^2 = N$. Under these assumptions and for SRRC pulse shaping filters, it is straightforward to verify that $\pi_I = (\mu_{I_1}^2 + \mu_{I_2}^2)\pi_d$.

We consider again the transmission of 1000 frames of 184 symbols, constant channels per frame, random channels from a frame to another, and we assume, for each frame, that ϕ_s, ϕ_{I_1}, ϕ_{I_2} and $\pi\tau_I/2T$ are independent random variables uniformly distributed on $[0, 2\pi]$, where ϕ_{I_1} are ϕ_{I_2} are the phases of the components $h_{I_1}(1)$ and $h_{I_2}(1)$, respectively. Under these assumptions, Fig. 10 shows, for $|\Delta_f|T = 0.50$ and 1, the variations of the SER at the output of the considered receivers for both R and QR signals, as a function of ϵ_s, for $N = 1$, $\omega = 0.5$, $\epsilon_I/\epsilon_s = 10$ dB and $\mu_{I_1} = \mu_{I_2}$. The conclusions of Fig. 8 hold for Fig. 10.

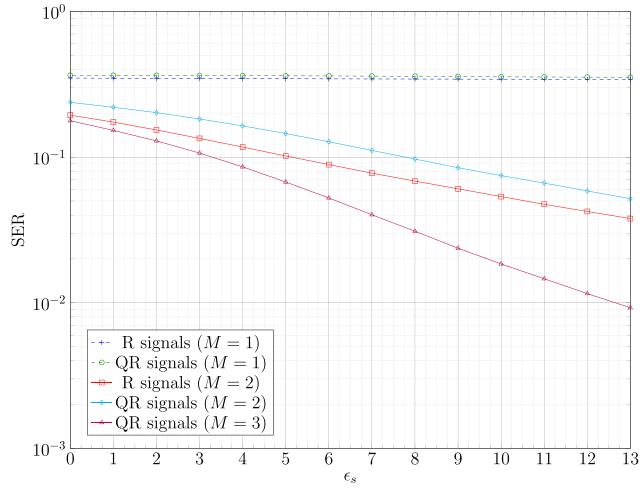

(a)

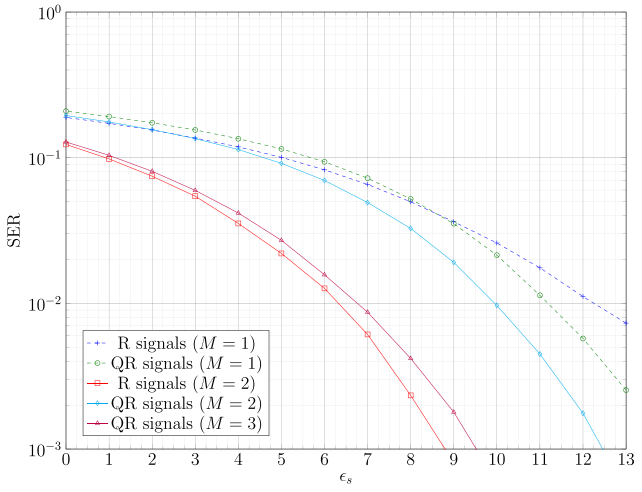

(b)

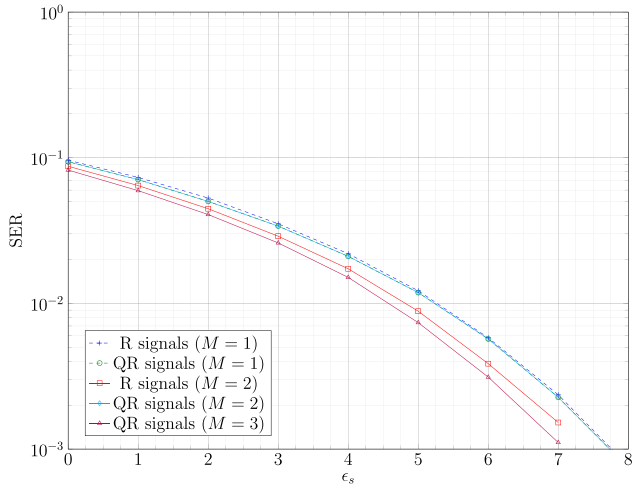

(c)

Fig. 8. SER as a function of ϵ_s for $N=1$, $\epsilon_I/\epsilon_s=10$ dB, $\omega=0.5$ deterministic one tap channels, R and QR signals, $|\Delta_f|T=0$ (a), $|\Delta_f|T=0.5$ (b) and $|\Delta_f|T=1$ (c).

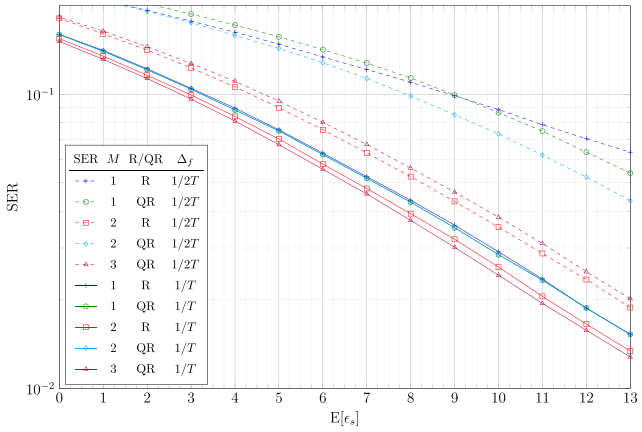

Fig. 9. ER as a function ϵ_s for N=1 ϵ_I/ϵ_s=10 dB, ω=0.5 Rayleigh fading one tap channels, R and QR signals, $|\Delta_f|T$=0.50 and 1.

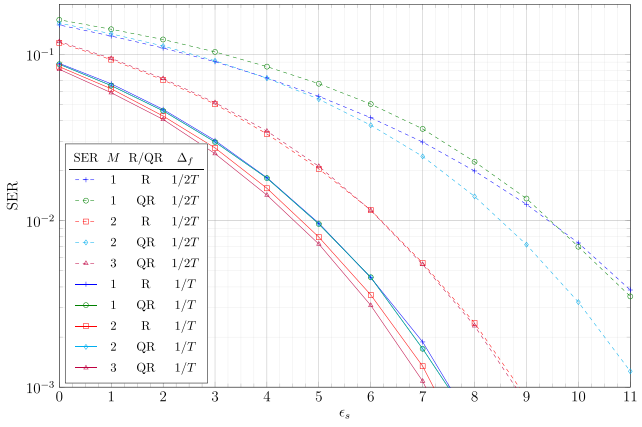

Fig. 10. SER as a function ϵ_s for $N=1$, $\epsilon_I/\epsilon_s=10$ dB, $\omega=0.5$, $\mu_{l_1}=\mu_{l_2}$ deterministic two-tap channels, R and QR signals, $|\Delta_f|T=0.50$ and 1.

6. Conclusion

The SAIC/MAIC concept has been extended in this paper, for arbitrary propagation channels and from a CT pseudo-MLSE based approach, to both R and QR signals with non-zero differential FO using WL FRESH filtering. For R signals, an extended two-input receiver has been proposed whereas for QR signals extended two and three-input receivers have been developed. Performance of the proposed receivers have been analyzed both analytically and by computer simulations, enlightening the impact of the FO on the performance. It has been proved that for arbitrary values of the FO, the extended two-input receiver is less powerful for QR signals than for R ones, which extends to signals with a non zero FO, the results of [38] valid for signals without any FO. Moreover, for QR signals and arbitrary value of the FO, the extended three-input receiver has been proved to be better than the extended two-input one. Roles of spatial, spectral and phase discrimination between the sources have been explained for each receiver from original analytical SINR expressions. It has been proved in particular that contrary to the conventional receiver, the proposed two and three-input WL FRESH receivers have good performance whatever the value of the FO, increasing with the number M of inputs. The results of the paper should open new perspectives and should contribute to develop new powerful WL receivers for data-like MUI and/or multipaths mitigation of radiocommunication links using QR signals with FO such as CNPC of UAVs, satellite-based AIS links or FBMC-OQAM networks in particular.

Declaration of Competing Interest

Authors declare that they have no conflict of interest.

Appendix A

Proof of (40)–(53):

Consider the case of QR signals for $M=2$. First note that the following three identities $\mathbf{x}^*_{QR_{F_2}}(-f)=\mathbf{J}\mathbf{x}_{QR_{F_2}}(f+\beta_0)$ and $\mathbf{g}^*_{QR_{F_2},\ell}(-f)=\mathbf{J}\mathbf{g}_{QR_{F_2},\ell}(f+\beta_0)e^{-i4\pi\Delta_f\ell T}$ from (13), $[\mathbf{R}^{0*}_{n_{F_2}}(-f)]^{-1}=\mathbf{J}[\mathbf{R}^0_{n_{F_2}}(f+\beta_0)]^{-1}\mathbf{J}$ from (30) with $\beta_0=2\Delta_f+1/2T$ imply from (17) that $i^{-\ell}y_{QR_2}(\ell)$ is real-valued and as a result $\mathrm{E}[z^2_{n,F_2}(m)]=\mathrm{E}|y^2_{n,F_2}(m)|$ in (21).

Otherwise for $v(f)=\sqrt{T}\mathbb{1}_{[-1/2T,+1/2T]}(f)$, the cyclic frequencies α_k reduce to the values $\{0,-1/T,+1/T\}$. Consequently the SINR (27) deduced from (21) can be written as:

$$\mathrm{SINR}_{QR_2}(m)=\frac{\pi_b[\int A_{0,m}(f)df]^2}{\int[A_{0,m}(f)+A_{\frac{-1}{T},m}(f)+A_{\frac{1}{T},m}(f)]df}, \tag{66}$$

where

$$A_{\alpha_k,m}(f)\overset{\text{def}}{=}\mathbf{w}^H_{F_2,m}(f+\frac{\alpha_k}{2})\mathbf{R}^{\alpha_k}_{n_{F_2}}(f)\mathbf{w}_{F_2,m}(f-\frac{\alpha_k}{2}). \tag{67}$$

Applying the matrix inversion lemma to $\mathbf{R}^0_{n_{F_2}}(f)$ deduced from (30):

$$[\mathbf{R}^0_{n_{F_2}}(f)]^{-1}=\frac{1}{N_0}\left(\mathbf{I}_{2N}-\frac{\mathbf{g}_{I_0,F_2}(f)\mathbf{g}^H_{I_0,F_2}(f)}{\|\mathbf{g}_{I_0,F_2}(f)\|^2+\frac{N_0T}{\pi_d}}\right), \tag{68}$$

we straightforwardly get from (19):

$$A_{0,m}(f)=\frac{\|\mathbf{g}_{QR_{F_2,m}}(f)\|^2}{N_0}\left(1-\frac{|\alpha_{s,I_{F_2,m}}(f)|^2}{1+\frac{1}{\epsilon_{I_F}(f)}}\right), \tag{69}$$

for $f\in B^0_F$ (where $B^{\alpha_k}_F$ denotes the set of frequencies f such that $\mathbf{g}_{QR_{F_2,m}}(f+\frac{\alpha_k}{2})$ is non-zero), $\alpha_{s,I_{F_2,m}}(f)\overset{\text{def}}{=}\mathbf{g}^H_{QR_{F_2,m}}(f)\mathbf{g}_{I_0,F_2}(f)/\|\mathbf{g}_{QR_{F_2,m}}(f)\|\|\mathbf{g}_{I_0,F_2}(f)\|$ and $\epsilon_{I_F}(f)\overset{\text{def}}{=}(\pi_d/N_0T)\|\mathbf{g}_{I_0,F_2}(f)\|^2$.

Then using (19) (68) and (30), we get after some algebraic manipulations for $\alpha_k\in\{-1/T,1/T\}$:

$$A_{\alpha_k,m}(f)=\frac{1}{N_0}\frac{\left(\alpha_{s,I_{F_2,m}}(f+\frac{\alpha_k}{2})\|\mathbf{g}_{QR_{F_2,m}}(f+\frac{\alpha_k}{2})\|^2\right)\left((\alpha_{s,I_{F_2,m}}(f-\frac{\alpha_k}{2})\|\mathbf{g}_{QR_{F_2,m}}(f-\frac{\alpha_k}{2})\|^2\right)}{\left((\epsilon^{1/2}_{I_F}(f+\frac{\alpha_k}{2})(1+\epsilon^{-1}_{I_F}(f+\frac{\alpha_k}{2}))\right)\left((\epsilon^{1/2}_{I_F}(f+\frac{\alpha_k}{2})(1+\epsilon^{-1}_{I_F}(f+\frac{\alpha_k}{2}))\right)} \tag{70}$$

for $f\in B^{1/T}_f\cap B^{-1/T}_f$.

For strong CCI ($\epsilon_I\gg 1$) and for which $\epsilon_{I_F}(f)\gg 1$, $\epsilon_{I_F}(f+1/2T)\gg 1$ and $\epsilon_{I_F}(f-1/2T)\gg 1$ for $f\in B^0_F\cap B^{1/T}_F\cap B^{-1/T}_F$ and for frequencies for which $\mathbf{g}_{I_0,F_2}(f)$ is not proportional to $\mathbf{g}_{QR_{F_2,m}}(f)$, i.e., such that $|\alpha_{s,I_{F_2,m}}(f)|\neq 1$, the comparison between (69) and (70) implies that $|A_{\alpha_k,m}(f)|\ll A_{0,m}(f)$ for $\alpha_k\in\{-1/T,1/T\}$ and (66) reduces to

$$\mathrm{SINR}_{QR_2}(m)\approx\pi_b\int A_{0,m}(f)df. \tag{71}$$

Using the expressions of $\|\mathbf{g}_{I_0,F_2}(f)\|^2$, $\|\mathbf{g}_{QR_{F_2,m}}(f)\|^2$ and $|\mathbf{g}^H_{QR_{F_2,m}}(f)\mathbf{g}_{I_0,F_2}(f)|^2$ in (69), we get after simple algebraic manipulations:

$$\mathrm{SINR}_{QR_2}(m)\approx\epsilon_s\left[2-|\alpha^2_{s,I}|\int\frac{c(f,\Delta_f,T,\kappa_{s,I,m})}{v^2(f-\Delta_f)+v^2(f-\Delta_f-\frac{1}{2T})+\frac{T}{\epsilon_I}}df\right], \tag{72}$$

with

$$\begin{aligned}&c\big(f,\Delta_f,T,\kappa_{s,I,m}\big)\\&\overset{\text{def}}{=}v^2(f)v^2\big(f-\Delta_f\big)+v^2\big(f-2\Delta_f-\tfrac{1}{2T}\big)v^2\big(f-\Delta_f-\tfrac{1}{2T}\big)\\&+2v(f)v\big(f-\Delta_f\big)v\big(f-2\Delta_f-\tfrac{1}{2T}\big)v\big(f-\Delta_f-\tfrac{1}{2T}\big)\cos 2\kappa_{s,I,m}.\end{aligned} \tag{73}$$

Noting that for $\Delta_f\in[0,1/T]$, $v^2(f)v^2(f-\Delta_f)=T^2\mathbb{1}_{[-1/2T+\Delta_f,1/2T]}(f)$, $v^2(f-2\Delta_f-\frac{1}{2T})v^2(f-\Delta_f-\frac{1}{2T})=T^2\mathbb{1}_{[2\Delta_f,1/T+\Delta_f]}(f)$ and $v(f)v(f-\Delta_f)v(f-2\Delta_f-\frac{1}{2T})v(f-\Delta_f-\frac{1}{2T})=T^2\mathbb{1}_{[2\Delta_f,1/2T]}(f)$, we have to distinguish the three domains [0,0.25], [0.25,0.5] and [0.5,1] for $|\Delta_f|T$ to compute the integral in (72). Then after tedious but simple computations, this integral is approximated for strong CCI by:

$$1+|\Delta_f|T+(1-4|\Delta_f|T)\cos^2\kappa_{s,I,m}\ \text{ for }\ |\Delta_f|T\leq 0.25, \tag{74}$$

$$\left(\frac{3}{2}-\big|\Delta_f\big|T\right)\ \text{ for }\ 0.25\leq|\Delta_f|T\leq 0.5, \tag{75}$$

$$2\left(1-\big|\Delta_f\big|T\right)\ \text{ for }\ 0.5\leq|\Delta_f|T\leq 1. \tag{76}$$

Plugging these expressions (74)–(76) into the integral of (72), we get (43)–(45). □

The expressions (41) and (42) of the SINR for R signals and $M=2$ are proved similarly. What about the derivation of the SINR (46) for QR signals and $M=3$, it is also similar, but with:

$$\begin{aligned}&\mathrm{SINR}_{QR_3}(m)\\&=\frac{2\pi_b[\int A_{0,m}(f)df]^2}{\int[A_{0,m}(f)+A_{\frac{-1}{T},m}(f)+A_{\frac{1}{T},m}(f)]df+\ \mathrm{Re}[\int[B_{\frac{-1}{2T},m}(f)+B_{\frac{1}{2T},m}(f)]df]}\end{aligned} \tag{77}$$

where $B_{\beta_k,m}(f)\overset{\text{def}}{=}\mathbf{w}^H_{F_3,m}(f+\frac{\beta_k}{2})\mathbf{C}^{\beta_k}_{n_{F_3}}(f)\mathbf{w}^*_{F_3,m}(f-\frac{\beta_k}{2})$ and where the terms $|A_{\alpha_k,m}(f)|$ and $|B_{\beta_k,m}(f)|$ are no longer negligible compared to $A_{0,m}(f)$ for strong CCI. □

Supplementary material

Supplementary material associated with this article can be found, in the online version, at doi:10.1016/j.sigpro.2021.108171.

CRediT authorship contribution statement

Pascal Chevalier: Conceptualization, Data curation, Formal analysis, Writing - original draft, Writing - review & editing, Validation. **Rémi Chauvat:** Conceptualization, Data curation, Formal analysis, Writing - original draft, Writing - review & editing, Validation. **Jean-Pierre Delmas:** Conceptualization, Data curation, Formal analysis, Writing - original draft, Writing - review & editing, Validation.

References

[1] W.M. Brown, R.B. Crane, Conjugate linear filtering, IEEE Trans. Inf. Theory 15 (4) (July 1969) 462–465.
[2] W.A. Gardner, Cyclic wiener filtering: theory and method, IEEE Trans. Commun. 41 (1) (Jan. 1993) 151–163.
[3] B. Picinbono, P. Chevalier, Widely linear estimation with complex data, IEEE Trans. Signal Process. 43 (8) (Aug. 1995) 2030–2033.
[4] P. Chevalier, Optimal array processing for non stationary signals, in: Proc. ICASSP, Atlanta (USA), May 1996, pp. 2868–2871.
[5] B. Picinbono, On circularity, IEEE Trans. Signal Process. 42 (12) (Dec. 1994) 3473–3482.

[6] D.P. Mandic, V.S.L. Goh, Complex valued nonlinear adaptive filters, Noncircularity, Widely Linear and Neural Models, Wiley, New York, 2009.
[7] P. Schreier, L.L. Scharf, Statistical signal processing of complex-valued data? The theory of Improper and Noncircular Signals, Cambridge University Press, 2010.
[8] T. Adali, P. Schreier, L.L. Scharf, Complex-valued signal processing : the proper way to deal with impropriety, IEEE Trans. Signal Process. 59 (11) (Nov. 2011) 5101–5125.
[9] Z. Ding, G. Li, Single-channel blind equalization for GSM cellular systems, IEEE J. Sel. Areas Commun. 16 (8) (Oct. 1998) 1493–1505.
[10] H. Trigui, D.T.M. Slock, Performance bounds for cochannel interference cancellation within the current GSM standard, Signal Proccess. Elsevier 80 (2000) 1335–1346.
[11] P. Chevalier, F. Pipon, New insights into optimal widely linear array receivers for the demodulation of BPSK, MSK and GMSK signals corrupted by non circular interferences - application to SAIC, IEEE Trans. Signal Process. 54 (3) (March 2006) 870–883.
[12] R. Meyer, W.H. Gerstacker, R. Schober, J.B. Huber, A single antenna interference cancellation algorithm for increased GSM capacity, IEEE Trans. Wirel. Commun. 5 (7) (July 2006) 1616–1621.
[13] M. Austin, SAIC and synchronised networks for increased GSM capacity? 3G Americas? SAIC Working Group, Sep. 2003.
[14] A. Mostapha, R. Kobylinski, I. Kostanic, M. Austin, Single antenna interference cancellation (SAIC) for GSM networks, IEEE Proc. Veh. Technol. Conf. 2 (Oct. 2004) 1089–1093.
[15] M.G. Vutukuri, R. Malladi, K. Kuchi, R.D. Koilpillai, SAIC receiver algorithms for VAMOS downlink transmission, in: Proc. 8th Int. Symp. Wireless Commun. Syst., Aug. 2011, pp. 31–35.
[16] W.H. Gerstacker, R. Schober, R. Meyer, F. Obernosterer, M. Ruder, H. Kalveram, GSM/EDGE: a mobile communications system determined to stay, Int. J. Electron. Commun. 65 (2011) 694–700.
[17] M. Ruder, R. Meyer, F. Obernosterer, H. Kalveram, R. Schober, W.H. Gerstacker, Receiver concepts and resource allocation for OSC downlink transmission, IEEE Trans. Wirel. Commun. 13 (3) (March 2014) 1568–1581.
[18] D. Molteni, M. Nicoli, Joint OSC receiver for evolved GSM/EDGE, IEEE Trans. Wirel. Commun. 12 (6) (June 2013) 2608–2619.
[19] W. Deng, Z. Li, Y. Xia, K. Wang, W. Pei, A widely linear MMSE anti-collision method for multi-antenna RFID readers, IEEE Commun. Lett. 23 (4) (Aug. 2019) 647–664.
[20] D.J. Nelson, J.R. Hopkins, Coherent demodulation of AIS-GMSK signals in co-channel interference, in: IEEE Asilomar Conf. on Circuits, Systems and Computers, Nov. 2011.
[21] G.M. Swetha, K. Hemavathy, S. Natarajan, V. Sambasiva, Overcome message collisions in satellite automatic ID systems, Microwave and RF, Systems, May 2018.
[22] O. Cherrak, H. Ghennioui, N. Thirion-Moreau, E.H. Abarkan, Blind separation of complex-valued satellite-AIS data for maritime surveillance : a spatial quadratic time-frequency domain approach, Int. J. Electr. Comput. Eng. (IJECE) (June 2019) 1732–1741.
[23] M. Bavand, S.D. Blostein, User selection and multiuser widely linear precoding for one-dimensional signalling, IEEE Trans. Veh. Technol. 67 (12) (Dec. 2018) 11642–11653.
[24] J.C. De Luna Ducoing, N. Yi, Y. Ma, R. Tafazolli, Using real constellations in fully-and over loaded large MU-MIMO systems with simple detection? IEEE Wirel. Commun. Lett. 5 (1) (Feb. 2016) 92–95.
[25] K.P. Valavanis, G.J. Vachtsevanos, Handbook of Unmanned Aerial Vehicles, Springer, New-York, NY, USA, 2015.
[26] Y. Zeng, R. Zhang, T.J. Lim, Wireless communications with unmanned aerial vehicles: opportunities and challenges, IEEE Commun. Mag. 54 (5) (May 2016) 36–42.
[27] Command and Control (C2) Data Link Minimum Operational Performance Standards (MOPS) (Terrestrial), Document RTCA-DO-362, RTCA Std., 2016,
[28] D. Darsena, G. Gelli, I. Iudice, F. Verde, Equalization techniques of control and non-payload communication links for unmanned aerial vehicles, IEEE Access 6 (2018) 4485–4496.
[29] B. Farhang-Boroujeny, R. Kempter, Multicarrier communication techniques for spectrum sensing and communication in cognitive radios, IEEE Commun. Mag. 46 (4) (Apr. 2008) 80–85.
[30] D. Chen, Y. Tian, D. Qu, T. Jiang, OQAM-OFDM for wireless communications in future internet of things: a survey on key technologies and challenges, IEEE Internet Things J. 5 (5) (Oct. 2018) 3788–3809.
[31] M. Caus, A.I. Perez-Neira, Comparison of linear and widely linear processing in MIMO-FBMC systems, in: Proc. Int. Symp. Wireless Commun. Syst., Ilmenau, Germany, Aug. 2013, pp. 21–25.
[32] M. Caus, A.I. Perez-Neira, Multi-stream transmission for highly frequency-selective channels in MIMO-FBMC/OQAM systems, IEEE Trans. Signal Process. 62 (4) (Feb. 2014) 786–796.
[33] Y. Chen, M. Haardt, Widely linear processing in MIMO FBMC/OQAM systems, in: Proc. Int. Symp. Wireless Commun. Syst., Ilmenau (Germany), Aug. 2013, pp. 743–747.
[34] S. Josilo, M. Narandzic, S. Tomic, S. Nedic, Widely linear filtering based kindred CCI suppression in FBMC waveforms, in: Proc. Int. Symp. Wireless Commun. Syst., Barcelona (Spain), Aug. 2014.
[35] A. Ishaque, G. Ascheid, Widely linear receivers for SMT systems with TX/RX frequency-selective I/Q imbalance, in: Proc. Int. Symp. Personal, Indoor Mobile Radio Commun., 2014, p. 800-805.
[36] K. Kuchi, Partial response DFT-precoded-OFDM modulation, Proc. Trans. Emerg. Telecommun. Technol. 23 (May 2012) 632–645.
[37] R.R.M. De Alancar, L.T.N. Landau, R.C. De Lamare, Continuous phase modulation with 1-bit quantization and oversampling using iterative detection and decoding, EURASIP J. Wirel. Commun. Netw. 1 (2020) 1–26.
[38] P. Chevalier, R. Chauvat, J.-P. Delmas, Enhanced widely linear filtering to make quasi-rectilinear signals almost equivalent to rectilinear ones for SAIC/MAIC, IEEE Trans. Signal Proces. 66 (6) (March 2018) 1438–1453.
[39] J.-P. Delmas, S. Sallem, P. Chevalier, Sensitivity of SAIC and MAIC concepts to residual frequency offsets, in: Proc. EUSIPCO, Alborg (Denmark), Aug. 2010.
[40] R. Chauvat, P. Chevalier, J.-P. Delmas, Widely linear FRESH receiver for SAIC/MAIC with frequency offsets, in: Proceedings. Int. Symp. Wireless Commun. Syst. (ISWCS), Brussels (Belgium), ISWCS, Aug. 2015.
[41] R. Chauvat, J.-P. Delmas, P. Chevalier, Two and three-inputs widely linear FRESH receivers for cancellation of a quasi-rectilinear interference with frequency offset, in: Proc. EUSIPCO, Budapest (Hungaria), Aug. 2016.
[42] H.E. Wong, J.A. Chambers, Two-stage interference immune blind equalizer which exploits cyclostationary statistics, Electron. Lett. 32 (19) (Sep. 1996) 1763–1764.
[43] G. Gelli, L. Paura, A.M. Tulino, Cyclostationarity-based filtering for narrow-band interference suppression in direct-sequence spread spectrum systems, IEEE J. Sel. Areas Commun. 6 (9) (Dec. 1998) 1747–1755.
[44] G. Latouche, D. Pirez, P. Vila, MMSE cyclic equalization, in: IEEE Mil. Commun. Conf., Boston, Oct. 1998, pp. 150–154.
[45] K. Zhou, S. Cao, R. Song, L. Zhang, Some blind fresh equalization algorithms with anti-interference capabilities, J. Electron. (China) 25 (6) (Nov. 2008) 768–773.
[46] A. Mirbagheri, K.N. Plataniotis, S. Pasupathy, An enhanced widely linear CDMA receiver with OQPSK modulation, IEEE Trans. Commun. 54 (2) (Feb. 2006) 261–272.
[47] W.A. Gardner, C.W. Reed, Making the most out of spectral redundancy in GSM: cheap CCI suppression, in: Proc. ASILOMAR, Pacific-Greove, 2001, pp. 883–889.
[48] A.U.H. Sheikh, F. Hendessi, FRESH-DFE: a new structure for interference cancellation, Wirel. Personal Commun. J. 44 (2008) 101–118.
[49] W.H. Gerstacker, R. Schober, A. Lampe, Receivers with widely linear processing for frequency-selective channels, IEEE Trans. Commun. 51 (9) (Sep. 2003) 1512–1523.
[50] P.A. Laurent, Exact and approximate construction of digital phase modulations by superposition of amplitude modulated pulses (AMP), IEEE Trans. Commun. 34 (2) (Feb. 1986) 150–160.
[51] J.G. Proakis, Digital communications, Mc Graw Hill Series in Electrical and Computer Engineering, fourth ed., 2001.
[52] D. Vucic, M. Obradovic, Spectral correlation evaluation of MSK and offset QPSK modulation, Signal Process. 78 (1999) 363–367.
[53] S. Sallem, J.-P. Delmas, P. Chevalier, Optimal SIMO MLSE receivers for the detection of linear modulations corrupted by non-circular interference, in: Proc. SSP, Ann Arbor, USA, Aug. 2012.
[54] G. Ungerboeck, Adaptive maximum likelihood receiver for carrier-modulated data transmission systems, IEEE Trans. Commun. 22 (5) (May 1974) 624–636.